The Synthesis of Nanoporous Hydrogels Using Sacrificial Block Copolymers

by
Jungmee Kang

B.S., Chemical Engineering
Pusan National University, 1996

M.S., Chemical Engineering
Pusan National University, 1998

Submitted to the Department of Chemical Engineering

In partial fulfillment of the requirements for the degree of

DOCTOR OF PHILOSOPHY IN CHEMICAL ENGINEERING

at the

MASSACHUSETTS INSTITUTE OF TECHNOLOGY

September, 2006

Signature of Author: ----------
Department of Chemical Engineering
July 21, 2006

Certified by: ----------
Kenneth J. Beers
Assistant Professor of Chemical Engineering
Thesis Supervisor

Accepted by: ----------
William M. Deen
Professor of Chemical Engineering
Chairman, Committee for Graduate Students

The Synthesis of Nanoporous Hydrogels Using Sacrificial Block Copolymers

by

Jungmee Kang

Submitted to the Department of Chemical Engineering on July 21, 2006 in partial fulfillment of the requirements for the degree of Doctor of Philosophy in Chemical Engineering

ABSTRACT

The purpose of this research is to synthesize nanostructured and porous hydrophilic networks (nanoporous hydrogels) using block copolymers and to understand their transport properties. Nanoporous materials are synthesized by connecting two or more chemically distinct polymer blocks, inducing microphase separation to form a pattern on the scale of tens of nanometers, and finally removing one of the polymer blocks. The sacrificial block needs to be degraded easily and controllably and the blocks must self-assemble. Desired properties for the non-degradable polymer block are that it be hydrophilic and that it can be crosslinked to form a hydrogel. Advantages of the nanoporous hydrogels are hydrophilicity and flexibility, and the hydrophilic nature would make these membranes suitable for the separation, based on size selectivity, of biological macromolecules such as proteins.

Hydrogels with nanoscale structure were synthesized using amphiphilic *poly*(ε-caprolactone-*b*-ethylene oxide-*b*-ε-caprolactone) (PCL-*b*-PEO-*b*-PCL) triblock copolymers. The triblock copolymer was produced by the ring opening polymerization of ε-caprolactone with PEO as a macro-initiator in the presence of stannous octoate as a catalyst. PCL and PEO have a sufficiently high segment-segment interaction parameter to induce microphase separation in bulk (the calculated χ_{FH} is 0.15 at 70 *°C*) or in water. PCL degrades easily in a NaOH aqueous solution. PEO is hydrophilic and crosslinkable by ultraviolet (UV) or other forms of ionizing radiation such as an electron beam or ^{60}Co. A pore size is controlled by the molecular weights of the block copolymers. Furthermore, terminal hydroxyl groups of PEO are restored after PCL removal that allow further chemical modification.

To search for optimum crosslinking conditions, PEO homopolymers were studied. Electron beam irradiation of up to 50 *Mrads* on PEO bulk films did not produce networks when the primary molecular weights of PEO were small. Gel fractions of electron beam crosslinked polymers increased when the primary molecular weight of PEO increased, but the produced M_c (molecular weight between crosslinks) values were too high to achieve fine mesh sizes. Therefore, aqueous solutions of PEO were studied to achieve lower M_c values (~ 1,500 *g/mol*).

Microstructures in aqueous solutions of PCL-PEO-PCL block copolymers were studied by Small Angle X-ray Scattering (SAXS). The SAXS studies show that the block copolymers form 30-40 *nm* structures in aqueous solution. Lamellar and cylindrical nanostructures were observed by SAXS, indicating cylindrical structure as the block lengths become more different in length. The lamellar structure remained after electron-beam crosslinking of the block copolymers as shown by Atomic Force Microscopy (AFM). It is demonstrated through Fourier Transform Infrared Spectroscopy (FTIR), mass loss, and

Differential Scanning Calorimetry (DSC) that the PCL can be completely removed by hydrolysis in NaOH(*aq*) to form porous PEO hydrogels. After PCL removal, the resulting nanoporous hydrogels have relatively high macromolecular diffusivities due to pores produced by PCL removal as observed in Fluorescence Recovery After Photobleaching (FRAP) studies.

The effect of temperature and water content on morphology of PCL-*b*-PEO-*b*-PCL, with block number average molecular weights of 9,000-30,000-9,000 *g/mol*, was also studied. Cylindrical morphology was observed in a solvent-evaporated sample. When it was heated above the melting peaks of both PEO and PCL blocks, a change in morphology was observed by SAXS. When this sample was cooled to room temperature in the ambient atmosphere, another morphology (lamellae) was observed with SAXS and AFM. This asymmetric change in morphology across the melting-crystallization transition suggests a role of kinetics (microphase separation and crystallization) in determining the observed microstructures. Addition of water at room temperature also affected the microphase separation of the block copolymer due to hydrophilicity of PEO. As the polymer concentration is decreased below 60%, the morphology changes from cylinders to lamellae. DSC shows that water addition decreases PEO crystallinity but PCL crystallinity remains.

These hydrogels retain active functional groups following PCL removal that serve as sites for further chemical modification with pH or temperature responsive materials, which may find use in drug separation and drug delivery systems.

Thesis Supervisor: Kenneth J. Beers
Assistant Professor of Chemical Engineering

Acknowlegements

When I stepped into my dorm at MIT for the first time, I was exhausted. It had been a long flight and everything was new. But when I looked at the beautiful night scenery of the Charles River and Boston out of the window, I was fascinated and forgot my tired body. Charms of Cambridge engulfed me and gave me one of the happiest moments in my life, until I was waken by the real life at the first Fall semester. I had heard that the first semester of a PhD course was the most difficult one, but I did not realize how difficult until I experienced one myself. Many people helped me go through numerous difficult times by giving me warm encouragement, advice, and help.

I thank my thesis advisor, Prof. Ken Beers, for his patience and insight. He was so friendly and nice that I could ask any questions without feeling embarrassed. I also thank Prof. Bob Cohen and Prof. Darrell Irvine for their encouragement and many helpful comments during thesis committee meetings. I learned a lot of helpful information for my research in their classes as well. I thank Prof. Alan Hatton for opening up his lab and supplying FRAP equipment.

I thank Mr. Ken Wright for the electron beam irradiation of many samples of mine. I also thank Juhyun Park, Daeyeon Lee, and Junsang Doh for their generous help on my FT-IR and SEM experiments. Tim McClure and Libby Shaw at CMSE helped me a lot as well. I thank Smeet Deshmukh for her help on laser alignment of FRAP equipment. Rachel Pytel and Brian Pete who answered all my questions about SAXS in a very friendly manner. I appreciate the time and effort of Kirill Titievsky who explained his computation work to me and helped me run simulations.

I was so lucky to have a wonderful first year class. Haring Tang and Luwi Oluwole, thank you for helping me open up my mind and become friends with many other people. Keith Tyo, thank you for the Bible studies, and I had a lot of fun when we were sailing together too. I also thank my lunch friends, Chong Gu and Naresh Chennamsetty, for introducing me to so many interesting things about China and India.

I thank my parents and sister for all their care, support, and encouragement. I miss you! I thank Gabor Erdodi for listening to me when I want to talk, giving me an advice when I need it, reviewing my papers when I needed feedback, and more. Thank you for being with me.

Table of Contents

List of Figures

List of Tables

List of Schemes

1. Background

1.1. Introduction

Nanostructured materials have patterns on the scale of tens of nanometers. To produce nanostructured materials, block copolymers have been used widely, employing the microphase separation between incompatible polymer blocks. Especially, nanoporous materials have attracted much interest for a wide variety of applications. Block copolymers of two or more chemically distinct polymer blocks self-assemble to form patterns on the scale of tens of nanometers. By removing a sacrificial block of the block copolymers, nanoporous materials are formed. Specifically, hydrophobic materials such as polystyrene have been used extensively for non-degradable blocks, and the high glass transition temperature (T_g) of polystyrene allows retention of the porous structures at room temperature. To remove the degradable block from the block copolymers, several degradation techniques have been used, including thermal degradation, ion etching, ozonolysis, and hydrolysis.

In the following, several examples of non-degradable polymers and degradable polymers are described in addition to the degradation techniques employed. They are categorized based on their possible applications.

1.2. Examples of nanoporous materials

- **Low dielectric materials for microelectronic devices**: Materials with low dielectric constants are useful in microelectronic areas for electronic isolation. For example, foamed polyimides were studied for this purpose (Hedrick, 1999). The voids need to be as small as possible to produce good isolation layers in the polyimide. Sub-micron sized voids are produced by the microphase separation of a thermally-decomposable polymer in a polyimide continuous phase. Widely used decomposable polymers are poly(propylene oxide), poly(methyl methacrylate), poly(styrene), poly(α-methylstyrene), poly(lactides) and poly(lactones). The typical degradation temperature is above 250°C, well below the thermal degradation temperatures of polyimides.

- **Nanolithography for microelectronic devices**: Traditional photolithography involves a mask and a photoresist, which makes it difficult to produce small patterns on the scale of nanometers that are much smaller than the wavelengths used. Alternative surface patterning methods were studied by Park (1997). Well-defined patterns from block copolymer self-assembly can be used to produce an etching mask for nanoelectronic devices. The patterns are on the scale of tens of nanometers. Polystyrene-polybutadiene (PS-PB) diblock copolymers were used to produce lithography templates. A PB phase forms spheres in the continuous PS matrix after annealing. The PB spheres are then transferred into holes or dots by two different processes. First, PB spherical phases can be degraded by ozonolysis to form holes because ozone breaks down the double bonds in PB. An alternative approach is to prevent PB from degrading by reactive ion etching to form nanodots.

- **Filters**: The final example is polystyrene monoliths. Nanoporous polystyrene materials were studied by Lee (1989) and Zalusky (2002). Polystyrene-*b*-poly D,L-lactide (PS-*b*-PDLLA) was used to induce cylindrical microphase separation, and the microstructure was aligned by a mechanical force such as a shear flow. After that, the PLA block was degraded by hydrolysis to produce pores (Zalusky, 2002). Crosslinkable polystyrene was also used (Lee, 1989). Isopropoxysilyl groups in PS are hydrolyzed to form silanol, which is followed by condensation of the silanols to form siloxane linkages. This crosslinking allows the nanopatterns to be retained in an organic solvent.

1.3. Objectives of our research

The purpose of our study is to synthesize nanostructured and porous hydrogel using block copolymers. Most of previously studied nanoporous materials involve hydrophobic polymer matrices and have not been crosslinked, therefore, the patterned porous structure will collapse upon exposure to a good (organic) solvent. Most of previously studied hydrogels were synthesized by homogeneous crosslinking of hydrophilic polymers, lacking

the advantage of anisotropic pore formation as in our approach. Hydrophilic materials that have nanopores produced by removal of one block in the block copolymers would make these materials suitable for biological applications such as protein separation and drug delivery because the hydrogels may not cause denaturation of biomaterials during separation processes, whereas hydrophobic membranes may cause this problem due to interaction with a hydrophobic core of the biomaterials.

In the following, various materials for synthesis of nanostructured and porous hydrogels are considered.

1.3.1 Materials selection

To produce nanostructured and porous hydrogels using block copolymers, the sacrificial polymer block needs to be degraded easily and selectively, and the non-degradable polymer block needs to be hydrophilic and crosslinkable. Polyethers and polyesters can be used as degradable blocks. Polymers of cyclic ethers can be used because of their low ceiling temperatures. For example, polytetrahydrofuran (PTHF) and poly(1,3-dioxolane) (PDXL) have relatively low ceiling temperatures: 80°C for PTHF (Ivin, 1984) and 0°C for PDXL (De Clercq, 1992). This is because its monomer is more stable thermodynamically, and they are depolymerized in the presence of a cationic initiator such as triflic acid (De Clercq, 1992). Other choices for the degradable block include polyesters such as poly(ε-caprolactone) (PCL) and poly(D,L-lactide) (PDLLA). Polyesters are hydrolyzed in acidic or basic aqueous solutions.

There are various examples of nondegradable polymer blocks such as poly(2-hydroxyethyl methacrylate) (PHEMA) and poly(ethylene oxide) (PEO). Poly(methyl methacrylate) (PMMA) is a hydrophobic polymer, but when it is hydrolyzed to produce carboxyl acid (Smith, 1993; Wang, 1991), it becomes hydrophilic. PEO has been reported to be crosslinked by UV in the presence of the photoinitiator, benzophenone (Doytcheva, 1997). These polymers were demonstrated to be crosslinkable under certain conditions by ionizing radiation such as an electron-beam (Dennison, 2001) or ^{60}Co (Nitta, 1958-59; Nitta, 1961; Salovey, 1963).

Poly(ε-caprolactone)-*b*-poly(ethylene oxide)-*b*-poly(ε-caprolactone) (PCL-PEO-PCL) block copolymers are selected for our research. The triblock copolymer can be produced by the ring opening polymerization of ε-caprolactone in the presence of PEO as a macro-initiator with a catalyst, stannous octoate. PCL and PEO have a sufficiently high segment-segment interaction parameter to induce microphase separation at above the melting points of both blocks (~70°C) (the calculated Flory-Huggins interaction parameter is 0.15 at 70°C). PCL degrades easily in a NaOH solution. PEO is hydrophilic and crosslinkable by ultraviolet (UV) or other forms of ionizing radiation such as an electron beam or ^{60}Co. Pore sizes are controlled by the molecular weights of the block copolymers. And terminal hydroxyl groups of PEO are restored when PCL-b-PEO-b-PCL is hydrolyzed that allow further chemical modification.

To produce the desired nanoporous hydrogels, it is essential to understand microphase separation behavior of block copolymers and the relationship between mesh size produced by crosslinks and the pore size produced by removal of a labile block in the block copolymer.

1.3.2. Microphase separation of block copolymers

Block copolymers that consist of incompatible blocks show several morphologies in the bulk phase, depending upon the volume fraction of one of the blocks (Matsen, 1994; Matsen, 1999; Bates, 1999). They show spherical, cylindrical, lamellar, or gyroid phase separation when $\chi_{FH}N$ is above 10.5, where χ_{FH} is a Flory-Huggins interaction parameter and N is a degree of polymerization. Generally, χ_{FH} can be estimated using solubility parameters as shown in Eq 1-1, that uses parameters obtained from group contribution calculations (Van Krevelen, 1976).

$$\chi_{FH} = \frac{<V>(\delta_A - \delta_B)^2}{RT} \qquad \text{Eq 1-1}$$

<V> is the average molar volume of repeat units of both blocks, δ_A is a solubility parameter of A block in the block copolymer, R is the ideal gas constant, and T is absolute temperature.

To control the size of microstructures induced by microphase sepearation, different molecular weights of polymers can be used. An increase in block length produces larger

microstructures (Zalusky, 2002). For example, a domain period (λ) of a lamellar morphology in the strong segregation regime is proportional to $N^{2/3}$ as shown Eq 1-2 (Bates, 1999).

$$\lambda \cong 1.03 a \chi_{AB}^{1/6} N^{2/3} \qquad \text{Eq 1-2}$$

where a is a statistical segment length.

Adding homopolymers or solvents to block copolymers also can affect the morphology. For example, adding PS homopolymers to diblock copolymer containing PS as one of the blocks changes lamellar or cylindrical morphologies to gyroid depending on polymer concentration and molecular weight (Winey, 1992). Another example is the addition of water to amphiphilic block copolymers as studied for PEO-poly(propylene oxide)-PEO (PEO-PPO-PEO) block copolymer systems (Wanka, 1994). Various morphologies including cubic, hexagonal, and lamellar microphases (Ivanova, 2000) were observed depending on the triblock copolymer composition, concentration, and temperature.

1.3.3. Pore size and mesh size

There are two kinds of pores in nanostructured and porous hydrogels when they are swollen in water, which will be denoted as meshes and pores respectively in the following. A "mesh" is the random opening of a chain-free region and is present as well in homogeneous hydrogels. A "pore" corresponds to a chain-free region that correlates to the domain of a degraded block in a self-assembled block copolymer phase. A mesh size is determined by chemical crosslinks (or M_c), therefore, the denser is crosslink density, the narrower is the mesh size. A pore size is determined by the size of degradable block, i.e., the longer is the degradable block, the bigger is the pore size. A schematic diagram of nanoporous hydrogels in an aqueous solution is shown in Figure 1.1. At relatively high crosslink density, the mesh size between crosslinks (ξ) is small, and penetrants should diffuse mainly through pores. Therefore, these materials can be used for membranes for separation of macromolecules, with an additional length scale governed by the self-assembled morphology.

The relation between the mesh size and the equilibrium degree of swelling of homogeneous polymeric networks is described as follows (Canal, 1989).

$$\xi = Q^{1/3} \left(\overline{r_o^2} \right)^{1/2} \qquad \text{Eq 1-3}$$

ξ is the mesh size, Q is the volume ratio of the swollen to the unswollen network at equilibrium. $\left(\overline{r_o^2}\right)^{1/2}$ is the unperturbed root-mean-square end-to-end distance between crosslinks, which is $(3M_c/M_o)^{1/2}C_\infty^{1/2}\,l$ for PEO (M_c=molecular weight between crosslinks, M_o=molecular weight of repeat unit, C_∞ is the characteristic ratio, and l is an average bond length). Eq 1-3 is not rigorously correct for our non-homogeneous systems because the swelling ratio (Q) is related to both the mesh size (ξ) and the pore size (d), but it can be used to estimate approximate mesh and pore sizes. For example, when M_c=1,500g/mol, Q=17 (data from our experiment), C_∞=4.0, l=1.5A, and M_o=44g/mol are assumed for PEO hydrogels (Sundararajan, 1996), ξ is estimated to be 7.8 nm. Even with this large mesh size, the macromolecular diffusivity of proteins and small particles would be reduced significantly if there were no larger "pores" corresponding to the domains of the degraded blocks. This is described by the following equation (Lustig, 1988; Canal, 1989).

$$D_{gel} \cong D_\infty\left(1-\frac{r}{\xi}\right)e^{\left[\frac{-1}{(Q-1)}\right]} \qquad \text{Eq 1-4}$$

D_{gel} is the diffusivity of a penetrant through the mesh of the hydrogel, D_∞ is the diffusivity in solution, and r is the penetrant size.

When ξ is 7.8 nm, r is 7 nm, and Q is 17, D_{gel} is 10 % of D_∞.

1.4. Thesis overview

The purpose of this research is to synthesize nanoporous hydrogels using PCL-*b*-PEO-*b*-PCL amphiphilic block copolymers and to understand their transport properties. Due to lack of crosslinkable functional groups in PEO, a high energy electron beam (2.5 MeV) was used to produce the crosslinks, which are important to fix the nanostructures produced by microphase separation of the block copolymers after removal of the degradable PCL blocks. This crosslink studies were performed with PEO homopolymers and are described in chapter 2. Using the optimum crosslinking conditions found in these experiments, nanoporous hydrogels were synthesized, as detailed in Chapter 3. Briefly, nanoporous hydrogels were produced by (1) synthesizing PCL-PEO-PCL block copolymers, (2) crosslinking the PEO block of the block copolymer in aqueous solutions at high

concentrations, and (3) degrading the PCL blocks by hydrolysis. Diffusion coefficients of various proteins in these nanoporous hydrogels then were studied, as described in Chapter 4. Morphologies of the block copolymers in water were found to be affected by block length ratio of PEO and PCL, water content, and temperature. The morphology studies are described in Chapter 5.

The study presented in chapter 3 was published in *Biomacromolecules*. The studies described in chapter 4 and 5 will be submitted to *Biomaterials* and *Polymer*, respectively.

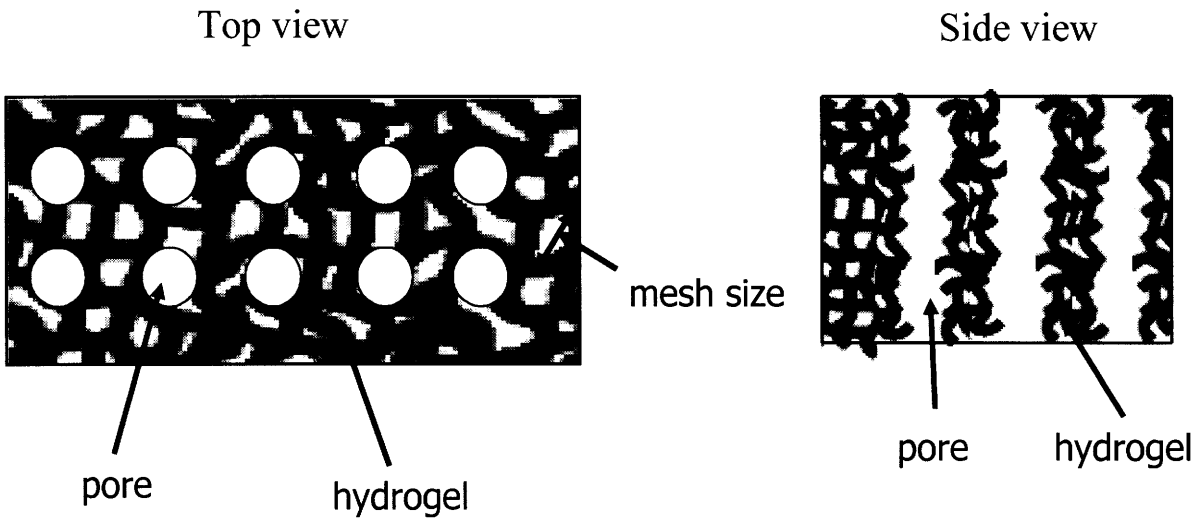

Figure 1.1. Schematic diagram of nanoporous hydrogel with cylindrical pores.

2. Crosslinking of PEO with electron beam irradiation

2.1. Introduction

PEO is hydrophilic and biocompatible, but lacks crosslinkable functional groups. However, for the synthesis of nanoporous hydrogels using PCL-*b*-PEO-*b*-PCL, PEO needs to be crosslinked after microphase separation to retain the nanostructures after PCL removal. Therefore, high energy irradiation including an electron beam (Doytcheva, 1997) and ^{60}Co (Nitta, 1958-59; Nitta, 1961; Salovey, 1963) can be used. These irradiation methods are not expected to crosslink PCL (Bovey, 1958). To our knowledge, no studies have been reported for PEO crosslinking by electron beam in the presence of PCL as done here. Therefore, it is necessary to make sure that PEO-PCL block copolymers can also be crosslinked using an electron beam, and to find the optimal crosslinking condition for this block copolymer.

In this chapter, the experimental results when bulk PEO films were irradiated with an electron beam are described followed next by the results using aqueous solutions of PEO. Finally, crosslinking studies for PEO-PCL diblock copolymers are described.

2.2. Experimental Section

2.2.1. Materials

Polyethylene oxide (PEO, M_n=4 600, 10 000, 47 000 g/mol) and benzophenone were purchased from Sigma-Aldrich and used without further purification. PEO-*b*-PCL (M_n=5000-4000 g/mol) diblock copolymers were obtained from Polymer Source, Inc. (Quebec, Canada) and used as received. Sodium azide (NaN_3) was purchased from Mallinckrodt, and solvents (benzene, dimethylene chloride, chloroform) were obtained from Aldrich (Milwaukee, WI).

2.2.2. Electron beam irradiation

For the electron beam irradiation of PEO in bulk, PEO was dissolved in dimethylene chloride, and PEO films were prepared to be 400 μm in thickness on Petri dishes 5 cm in

diameter. They were dried in hood for 1 day and in a vacuum oven for another day at room temperature. Electron beam irradiation was carried out at the High Voltage Research Laboratory at MIT. A 2.5 MeV van de Graff generator with the dose rate of 1.25 Mrad/pass and a belt speed of 0.8 cm/s was used. PEO bulk films were preheated for 20~30 min at 100°C before they were put on the belt of the electron beam generator to melt the crystalline PEO and to increase the amorphous portion, where most crosslinking takes place. For the electron beam irradiation of PEO in water, PEO was dissolved in Milli-Q water with 0.01% NaN_3 to retard bacterial growth. Aqueous PEO solutions were prepared to be 0.2 cm or 0.5 cm thick, and they were irradiated without preheating. Gel fractions were measured by comparing dry weights before and after extraction with Milli-Q water with 0.01% NaN_3.

2.2.3. Intrinsic viscosity measurement

Intrinsic viscosity of polymers was measured with benzene as a solvent at 25°C. An Ubbelohde viscometer (Cole-Parmer, size OC) was immersed in a constant temperature water bath (Koehler instrument). The retention time of all samples was measured after at least 10 minutes of temperature equilibration. The following equations (Eq. 2-1) were used to calculate intrinsic viscosities (Collins, 1973).

$$\frac{\eta_{sp}}{c} = [\eta] + k'[\eta]^2 c \qquad \text{Eq. 2-1}$$

$$\frac{(\ln \eta_r)}{c} = [\eta] + k''[\eta]^2 c$$

where η_r = relative viscosity = (retention time of a solution)/(retention time of pure solvent)

η_{sp} = specific viscosity = η_r -1

c = concentration in units of g/dl

$[\eta]$ = intrinsic viscosity in units of dl/g

k', k'' = constants ($k' - k'' \sim 0.5$ when experiments are performed correctly)

2.2.4. Swelling experiments.

For the samples that were irradiated in bulk, M_c (molecular weight between crosslinks) was measured in chloroform at room temperature after one day of equilibration. For the samples that were crosslinked in aqueous solution, 0.01% NaN3 in Milli Q water was used and the weights of the samples were measured at room temperature after two days' equilibration. The weights of the dry samples were measured after vacuum drying at 40°C for two days. M_c was calculated by either Eq. 2-2 or Eq. 2-3. Eq. 2-2 was used for the samples crosslinked in bulk film (Doytcheva, 1997).

$$\frac{1}{M_c} = \frac{2}{M_n} - \frac{\ln(1-v_{2s}) + v_{2s} + \chi_1 v_{2s}^{\ 2}}{V_1 \rho_2 (v_{2s}^{\ 1/3} - v_{2s}/2)} \qquad \text{Eq. 2-2}$$

$$\chi_1 = \frac{V_1(\delta_s - \delta_p)^2}{RT} + 0.34$$

where v_{2s}: polymer volume fraction at equilibrium swelling

V_1: molar volume of solvent=80.12 cm^3/mol for chloroform

ρ_2: polymer density

δ_s: solubility parameter of a solvent = 9.3 $(cal/cm^3)^{0.5}$ for chloroform

δ_p: solubility parameter of a polymer = 10.3 $(cal/cm^3)^{0.5}$ for PEO

χ_1: Flory-Huggins interaction parameter = 0.477 at 21°C

Eq. 2-3 was used for crosslinked samples in aqueous solutions (Dennison, 1986). This equation is more complicated than Eq. 2-2 because water is present during crosslinking experiments. Furthermore, χ values cannot be calculated from solubility parameters because water forms hydrogen bonds with PEO. Dennison (1986) obtained the χ value between PEO and water using osmometry.

$$\frac{1}{M_c} = \frac{2}{M_n} - \frac{\left(\frac{v}{V_1}\right)\left[\ln(1-v_{2s}) + v_{2s} + \chi_1 v_{2s}^{\ 2}\right]}{v_{2r}\left[\left(\frac{v_{2s}}{v_{2r}}\right)^{1/3} - \frac{1}{2}\left(\frac{v_{2s}}{v_{2r}}\right)\right]} \qquad \text{Eq. 2-3}$$

$$v_{2r} = \frac{w_p}{w_p + \left(\frac{\rho_p}{\rho_s}\right)(w_r - w_p)}$$

$$v_{2s} = \frac{w_p}{w_p + \left(\frac{\rho_p}{\rho_s}\right)(w_s - w_p)}$$

where, M_n : number average primary polymer molecular weight

v : polymer specific volume

V_1 : molar volume of solvent

χ_1 =F-H interaction parameter=0.426 between water and PEO at room temperature

v_{2s} : polymer volume fraction at equilibrium swelling

v_{2r} : polymer volume fraction immediately after crosslinking

w_r : weight of the gel immediately after crosslinking

w_s : weight of the fully swollen gel

w_p : weight of the dried polymer network

ρ_p : density of polymer

ρ_s : density of solvent

2.3. Results and Discussion

2.3.1. Electron beam irradiation of PEO in bulk

PEO with various molecular weights (M_n, 4 600, 10 000, 47 000 g/mol) was irradiated with an electron beam in bulk films. When PEO (4 600 g/mol) was irradiated with 50 Mrads in air, the intrinsic viscosity decreased to 0.113 dl/g from 0.129 dl/g (no irradiation), which indicates that chain scission may be predominant over crosslinking through the oxidation of the PEO main chain. When irradiated in an argon atmosphere, intrinsic viscosities increased slightly. Higher molecular weight PEO showed higher intrinsic viscosities than PEO of lower molecular weight (Figure 2.1). We also found that when the higher molecular weight (47 000 g/mol) of PEO was used, a dosage of 30 Mrads was sufficient for gelation, but it was not enough for the gelation of PEO 4600 g/mol. This is because a larger number of crosslinks (lower M_c values) is necessary for low MW PEO to

ensure that each chain has enough crosslinks to tie it into a network of other chains. At above a gelation dose, the effect of electron beam dose on gel fraction and M_c was studied, and the result is plotted in Figure 2.2. Higher doses produced higher gel fractions and lower M_c values.

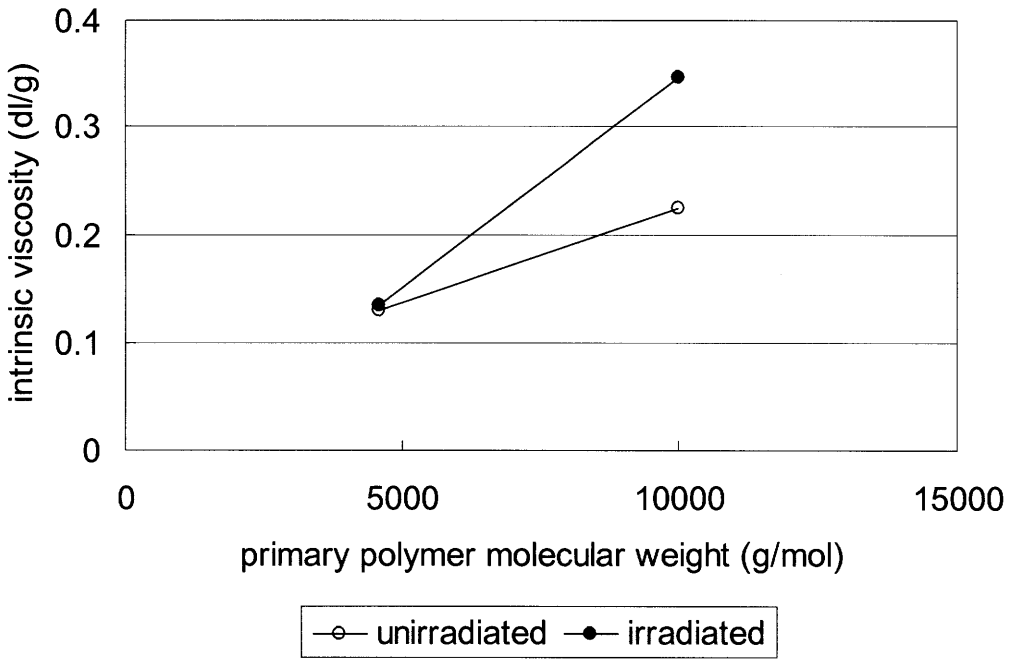

Figure 2.1. Effect of the molecular weight of PEO on the intrinsic viscosity after electron beam irradiation with 30Mrads dose in at argon atmosphere; the higher molecular weight of PEO (47 000g/mol) formed a gel with the 30 Mrads dose.

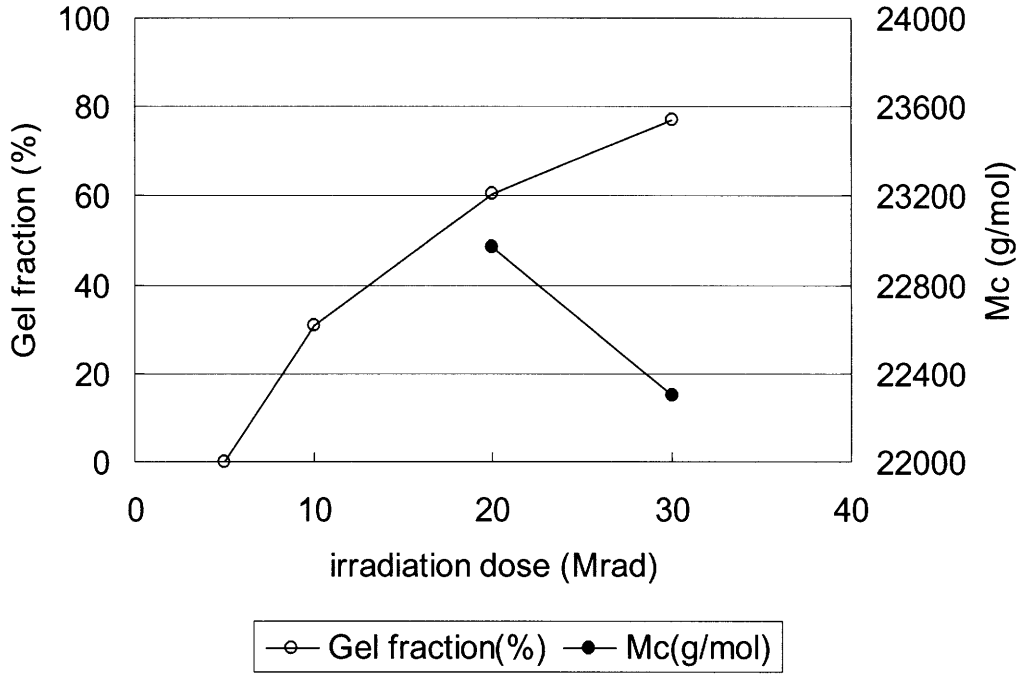

Figure 2.2. Effect of electron beam dose on gel fraction and M_c when PEO whose primary M_n is 47 000 g/mol was irradiated in an argon environment.

The gelation dose for PEO 47 000 g/mol is about 5 Mrads, and the gelation dose for M_n 10,000 g/mol is expected to be around 50 Mrads. Therefore, at least 50 Mrads is expected to be needed to produce mechanically stable hydrogels. But higher doses than 50 Mrads are not practically convenient to achieve. Therefore, we tried adding benzophenone into the PEO bulk films to increase crosslink densities. As shown in Scheme 2.1, benzophenone has been known to produce PEO radicals when they are added to PEO films undergoing ultraviolet (UV) irradiation, and PEO radicals react with other PEO radicals to form crosslinks (Doytcheva, 1997). However, benzophenone did not improve crosslinking on our samples as shown in Figure 2.3. Therefore, we considered adding water to improve crosslink density. The experimental results of how water affected M_c are described below.

2.3.2. Electron beam irradiation of PEO (10,000 g/mol) in water

It has been reported that water produces OH radicals and O anion radicals under an electron beam, and that they react with the PEO backbone to form PEO radicals (Dennison, 1986; Scheme 2.2). These PEO radicals react each other to undergo crosslinking. Therefore, the presence of water expected to enhance crosslink density. As shown in Figure 2.4, even with such small doses as 5, 10, and 20 Mrads, M_c values of 1500~4000 g/mol were achieved when PEO 10 000 g/mol was irradiated in a 9% aqueous solution. And after 20 Mrads, M_c reached an asymptotic value of 1,500 g/mol.

Various concentrations were also tested to see the concentration affects M_c, and the results are shown in Figure 2.5. M_c increased with an increase in concentration. 20 Mrad and 30 Mrad doese produced roughly similar M_c values.

The effect of sample thickness on the crosslinking of PEO was also studied. The 2.5 MeV van de Graff generator at the High Voltage Research Lab at MIT is known to be able to irradiate uniformly samples of up to 0.5 cm in thickness (Dennison, 1986). To identify the optimal sample thickness for our samples, two thicknesses (0.2 cm and 0.5 cm) of aqueous PEO solutions were studied. As shown in Figure 2.6, the two thicknesses did not produce very different M_c values. However, 0.2 cm produced more uniform M_c values. Therefore, this thickness was used in all further experiments where a specific thickness is not mentioned.

Scheme 2.1. Crosslinking of PEO induced by benzophenone and ultraviolet irradiation (Doytcheva, 1997).

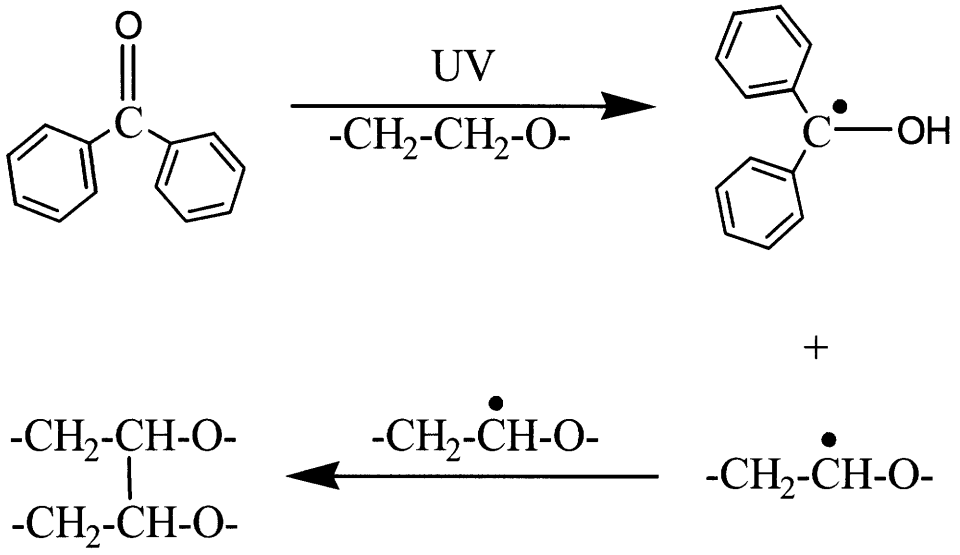

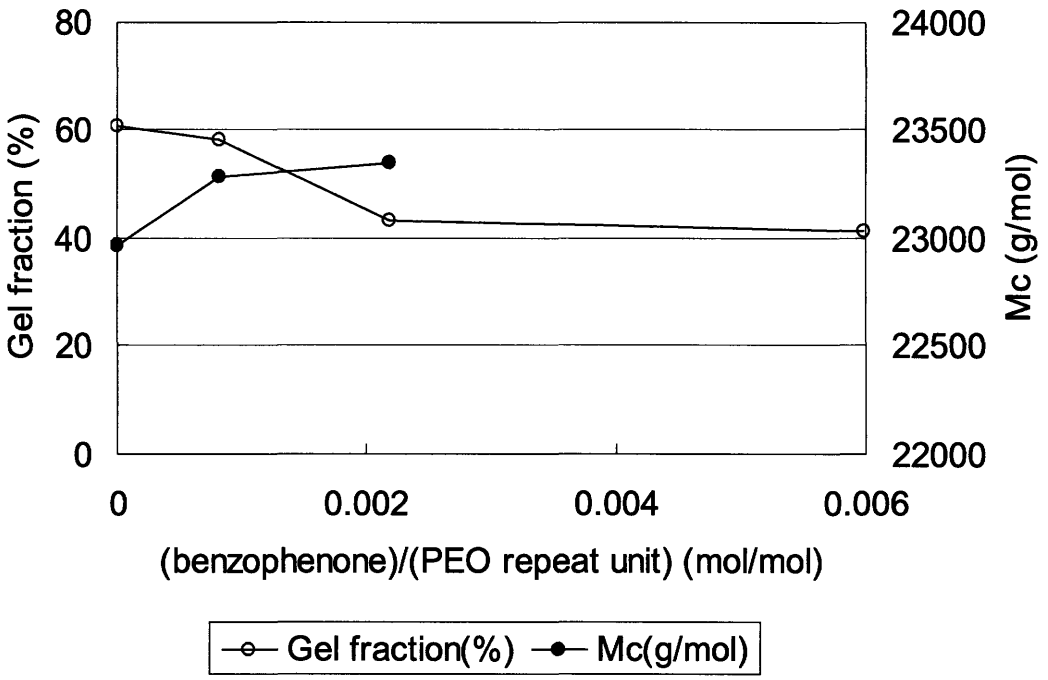

Figure 2.3. Effect of benzophenone on gel fraction and M_c when PEO whose primary molecular weight is 47 000 g/mol was irradiated with 20 Mrads in an argon atmosphere.

Scheme 2.2. Irradiation chemistry of PEO in water (image from Dennison, 1986).

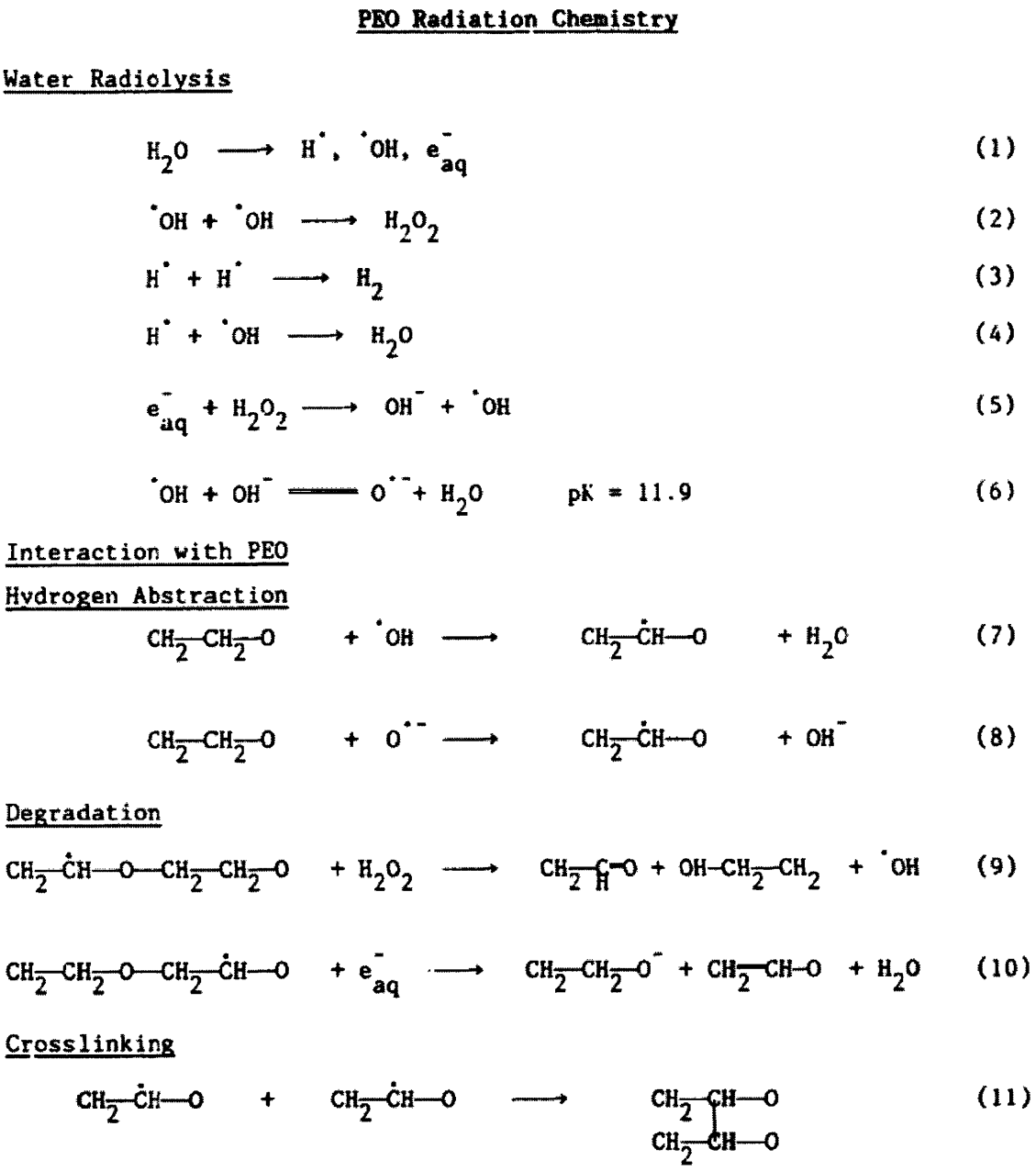

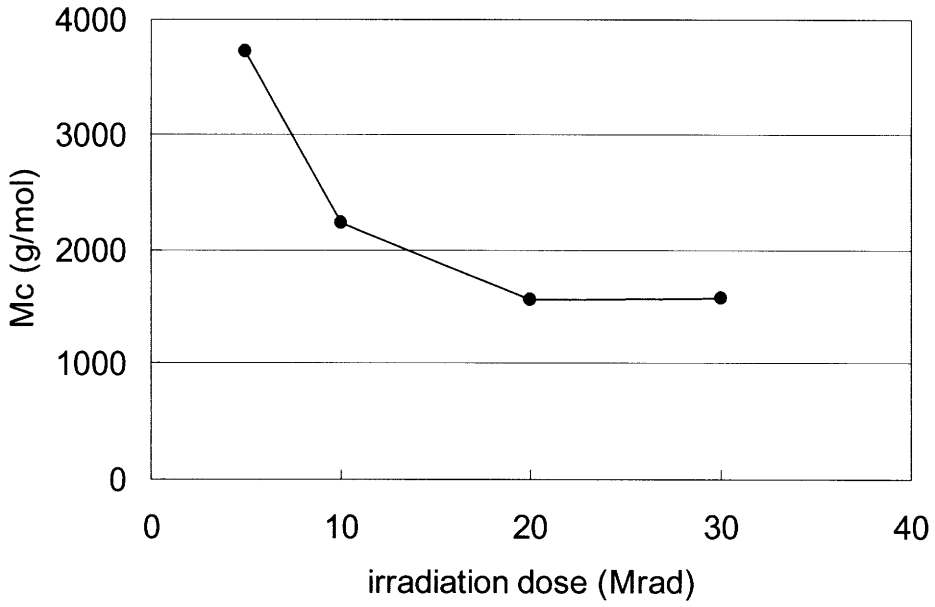

Figure 2.4. Effect of electron beam dose on M_c with a 9% PEO aqueous solution (PEO primary M_n=10 000g/mol).

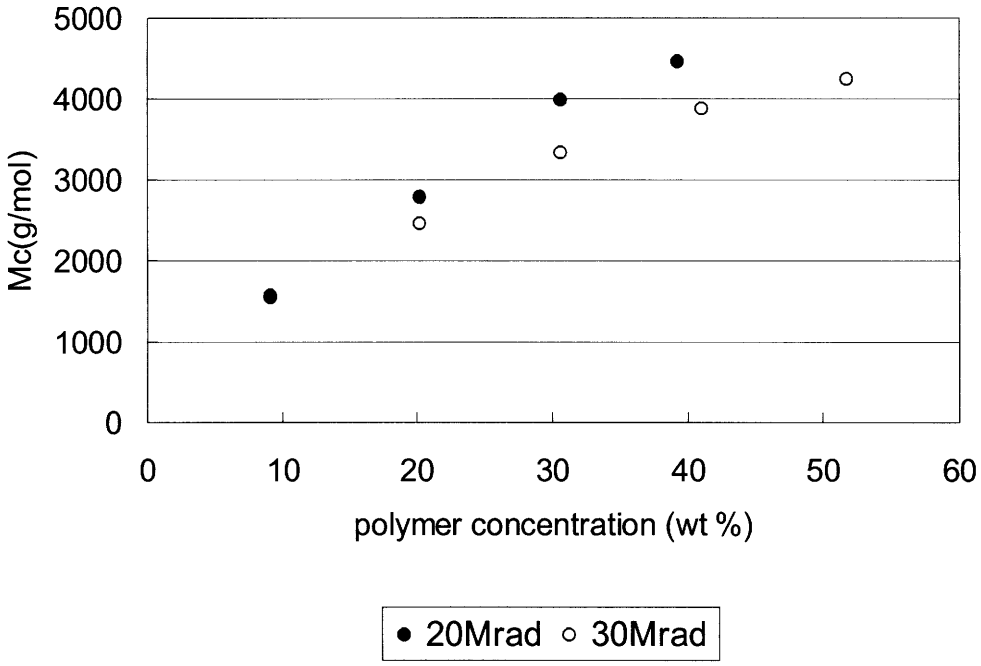

Figure 2.5. Effect of concentration in aqueous PEO solutions on M_c (primary PEO molecular weight is 10 000 g/mol).

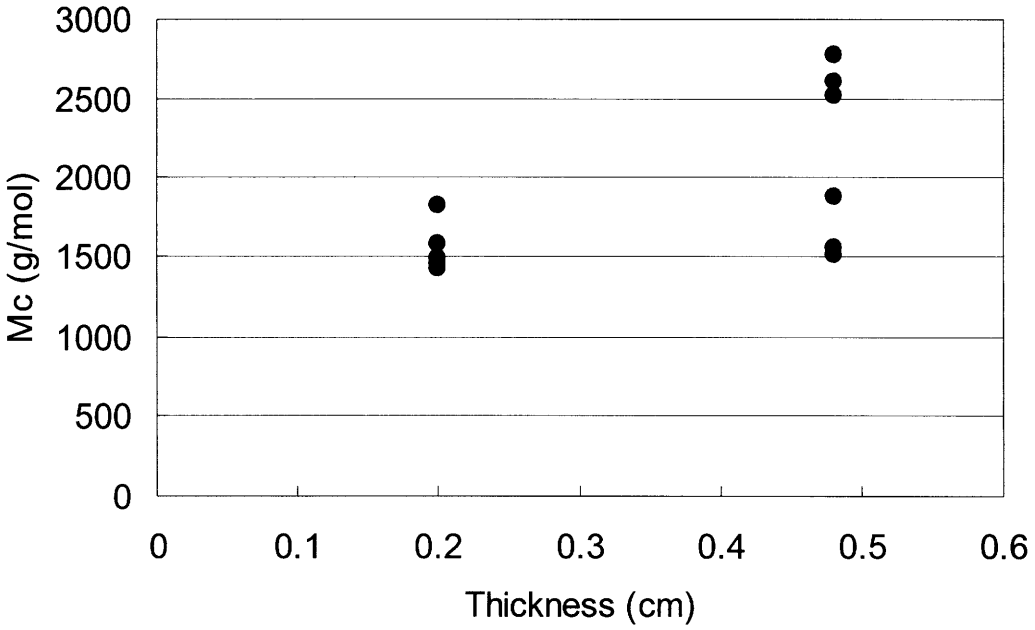

Figure 2.6. Effect of solution thickness on M_c when a 9% aqueous PEO solution (primary M_n=10 000 g/mol) was crosslinked with 20 Mrads.

2.3.3. Electron beam irradiation of PEO-*b*-PCL diblock copolymer in water

Crosslinking of diblock copolymers with an electron beam was studied first using a commercially available PEO-PCL diblock copolymer (M_n = 5000-*b*-4000 g/mol). Since we want to crosslink PEO and degrade PCL, PCL should contain enough ester linkages for hydrolysis after electron beam irradiation, and not impede PEO crosslinking. Bovey (1958) studied the crosslinking of polyesters in bulk, $-[(CH_2)_4COO]_n-$, and concluded that it required fairly high doses to form a gel and that the more CH_2 groups between ester functional groups, the easier crosslinking will occur. Since PCL has only five CH_2 groups between ester groups, it is expected that PCL does not undergo severe crosslinking under the current electron beam irradiation conditions. Furthermore, since water radiolysis accelerates the crosslinking process considerably, the hydrophobic PCL domain is even less favored than PEO for crosslinking by electron beam irradiation. Gel fraction data after electron beam irradiation of diblock copolymer aqueous solutions indicate that PEO is crosslinked in spite of presence of PCL (Figure 2.7). However, the polymer concentrations affect gel fraction. This further confirms that water is essential to crosslink PEO efficiently by an electron beam. Electron beam irradiation of block copolymers is described in more detail in Chapter 3.

2.4. Conclusions

Crosslinking experiments in the bulk PEO films were less effective than in aqueous solutions, and water increased the crosslink density remarkably to produce M_c values of about 1,500 g/mol. Crosslinking experiments with PEO-PCL diblock copolymers were performed successfully with the optimal experimental conditions that were achieved by the PEO experiments. Synthesis of nanoporous hydrogels using PEO-PCL block copolymers is further described in the next chapter.

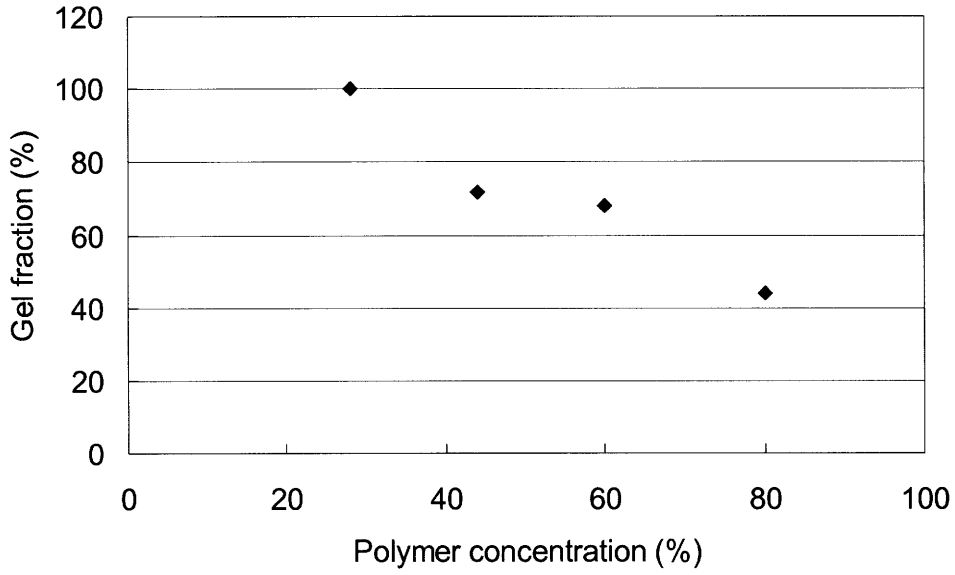

Figure 2.7. Effect of polymer concentration on the gel fraction of PEO-PCL diblock copolymer (5000-4000 g/mol) after crosslinking in water by an electron beam.

3. Synthesis and Characterization of PCL-*b*-PEO-*b*-PCL Based Nanostructured and Porous Hydrogels

3.1. Introduction

Nanoporous materials have received much attention due to their well-ordered nano-scale pore structures and their high surface areas, and have been studied for numerous potential applications in separation, catalysis, nanolithography, and as low dielectric materials. While inorganic nanoporous materials synthesized with metal oxides are hydrophilic, the majority of current nanoporous organic materials are hydrophobic, which limits potential biomedical applications. In this chapter, we report a novel synthetic method for hydrophilic, flexible, nanostructured and porous polymer networks.

Nanoporous materials derived from block copolymers are advantageous for the degree of control over pore size distribution that they offer. These materials are synthesized by connecting two or more chemically-distinct polymer blocks, inducing microphase separation to form a pattern on the length scale of tens of nanometers, and removing one of polymer blocks to generate voids. Polymers with high glass transition temperatures (T_g) have been used for the non-degradable blocks because a high T_g offers retention of structure at mild temperatures in spite of the absence of chemical cross-links (Hedrick, 1999; Park, 1997; Zalusky, 2002). However, once the glass melts or contacts a good solvent, such porosity disappears. This problem can be avoided by cross-linking a non-degradable block as shown by Lee (1989) and Cavicchi (2004).

Amphiphilic polymer networks (APNs) have been studied extensively for biological applications due to the presence of both hydrophilic and hydrophobic domains (Patrickios, 2003). Specifically, Barakat (1999) synthesized APNs using block copolymers of polyester and *poly*(2-hydroxyethylmethacrylate) (PHEMA), and studied hydrophilic and hydrophobic drug release profiles as the networks are swollen in hydrophilic and hydrophobic solvents. Another recent example is a *poly*(ethylene oxide)-*poly*(dimethyl siloxane) (PEO-PDMS)

network that can be used in contact lenses due to its optical clarity when swollen in water and to its high oxygen permeability (Erdodi, 2005). Hentze(1999) also used PEO as a hydrophilic domain in their study of a PEO-*b*-*poly*(butadiene) network. They induced microphase separation of the diblock copolymer in water to produce lamellar and cylindrical microstructures and then fixed the ordered structures by ^{60}Co radiation-induced cross-linking. In our study, an APN system is used to produce nanostructures in water, but instead of using the hydrophobicity of the hydrophobic domain as in the examples above, it is removed to produce a nanoporous hydrophilic network.

In this study, PCL-*b*-PEO-*b*-PCL block copolymers were selected. As shown by Bae(2005), these block copolymers show different microstructures by micellization in water depending upon the polymer concentration (Wanka, 1994) and the temperature. The molecular weights of the blocks also affect the phase structure (Bates, 1999). The copolymers must be cross-linked prior to void formation in order to retain any spatial structure originating from block copolymer templating. PEO can be cross-linked by an electron beam (Dennison, 1986), by UV (Doytcheva, 1997) or by a ^{60}Co source (Nitta, 1958-59; Nitta, 1961; Salovey, 1963). Here, an electron beam is used to cross-link the polymer through covalent C-C bonds, such that the resulting cross-links do not degrade once the PCL blocks are removed through hydrolysis of PCL's ester linkages in NaOH(*aq*) (Zalusky, 2002). The terminal hydroxyl groups of PEO are restored after the PCL is removed through hydrolysis, allowing later chemical modification. Due to their hydrophilicity and biocompatibility, the resulting nanoporous PEO networks may find use as hydrogels for selective separation or drug delivery.

3.2. Experimental Section

3.2.1. Materials.

PEO, ε-caprolactone, and stannous octoate were purchased from Sigma-Aldrich and used without further purification. PEO-*b*-PCL diblock copolymer (M_n=5,000-4,000 *g/mol*) was purchased from Polymer Source (Quebec, Canada). Sodium azide and methanol were

purchased from Mallinckrodt (Phillipsburg, NJ), and the solvents (dichloromethane, *n*-hexane) were obtained from EMD Chemicals (Gibbstown, NJ).

3.2.2. Synthesis of PCL-*b*-PEO-*b*-PCL triblock copolymers

PEO was reacted with ε-caprolactone in the presence of stannous octoate as a catalyst at 130°C for 21 hours under a nitrogen atmosphere. Synthesized block copolymers were dissolved in dichloromethane and precipitated into cold *n*-hexane three times to remove unreacted monomers, and the final products were dried in a hood at room temperature for one day and in a vacuum oven at 40°C for another two days. Three different triblock copolymers were synthesized using different molecular weights of the PEO macro-initiator.

3.2.3. Cross-linking of PCL-*b*-PEO-*b*-PCL by electron beam irradiation

PCL-*b*-PEO-*b*-PCL was dissolved in Milli-Q water in a 5 *cm* Petri dish in diameter, with 0.01% NaN_3 added to retard bacterial growth. After equilibrating the aqueous solutions at room temperature for one week, e-beam irradiation was carried out at the High Voltage Research Laboratory (HVRL) at MIT, using a 2.5 *MeV* van de Graff generator with a dose rate of 1.25 *Mrad/pass* and a belt speed of 0.8 *cm/s*. The temperature was not controlled during irradiation. For an emulsion at 20% polymer concentration, a 30 *Mrad* dose was used, while 50 *Mrad* doses were used at 40, 60, and 80% polymer concentrations. The maximum film thickness achievable with little depth variation in the electron dose is ~0.5 *cm* (Dennison, 1986), and our samples were approximately 0.2 *cm* thick. After cross-linking, the samples were extracted with 0.01% NaN_3 Milli-Q water, and the final products were dried in a vacuum oven at 40°C for two days. Dry weights of samples before and after extraction were compared to calculate the gel fractions.

3.2.4. Synthesis of nanostructured and porous PEO hydrogel

Cross-linked samples of PCL-*b*-PEO-*b*-PCL were placed in 40/60 (v/v %) methanol/water solutions with 0.5*M* NaOH at 100°C for two days to hydrolyze the ester

linkages of the PCL blocks. The degradation was followed by extraction with 40/60 (v/v %) methanol/water solutions and pure water to remove the degraded PCL monomer and oligomer segments. The final products were dried in a vacuum oven at 40°C for two days.

3.2.5. Esterification of the nanostructured and porous PEO hydrogel

The porous PEO hydrogels produced by the PCL degradation were reacted with an excess amount of glutaric acid at 100°C for one hour in the presence of concentrated sulfuric acid as a catalyst and 3Å molecular sieves for absorption of the water by-product. As a reference sample in which no esterification was to be expected, the same reaction condition was used except that toluene was added instead of glutaric acid. The reacted PEO hydrogels were extracted with dichloromethane and water.

3.2.6. Characterization

Number and weight average molecular weights (M_n and M_w, respectively) and polydispersities (M_w/M_n) were obtained with a Waters Gel Permeation Chromatograph (GPC) at the University of Akron using tetrohydrofuran (THF) as the solvent at a 1 *ml/min* elution rate with calibration through use of polystyrene standards. Proton Nuclear Magnetic Resonance (^{1}H-NMR) spectra were acquired by a 300 *MHz* Varian Mercury apparatus using $CDCl_3$ as a solvent at the MIT Department of Chemistry Instrumentation Facility (DCIF). Small Angle X-ray Scattering (SAXS) experiments were performed at the Institute for Soldier Nanotechnologies (ISN) at MIT, and Ultra Small Angle X-ray Scattering (USAXS) was conducted by a University-National laboratory-Industry Collaborative Access Team (UNICAT) at the Argonne National Laboratory. Wet samples of triblock copolymers (emulsions in water, cross-linked polymer hydrogels, and porous hydrogels after PCL removal) were enclosed or mounted upon Kapton™ tape. SAXS data were collected for exposures of 1,000 *sec* at room temperature. Background calibration was performed by subtracting the signals from the corresponding empty Kapton™ tape holders. Atomic Force Microscopy (AFM) images were taken with a Veeco Metrology Group Nanoscope IV Scanning Probe Microscope (Digital Instruments) at the MIT Center for Material Science and

Engineering (CMSE). Dry samples were microtomed to produce smooth surfaces for AFM measurement. Fourier Transform Infrared Spectroscopy (FTIR) measurements were conducted using a Nicolet Magna 860 at CMSE. Samples for IR measurement were vacuum-dried at 40°C for at least two days prior to analysis and prepared by the following methods: (1) by grounding a dried sample with mortar and pestle, mixing with KBr powders, (2) by crushing a dry sample to form a thin film on a ZnSe plate, or (3) by making thin film using diamond compression cell windows. Melting points (T_m) of block copolymers were obtained with a Perkin Elmer Pyris 1 Differential Scanning Calorimeter (DSC) at CMSE. Wet samples of 5-10 *mg* were used for DSC, and high pressure stainless steel pans with O-rings were used to prevent evaporation of water. The samples were heated at the rate of 10°C/*min* from 20°C to 100°C and cooled at the rate of 10°C/*min* to 20°C to erase prior thermal history. These samples were heated again to 100°C at the same rate to collect the DSC results.

3.3. Results and Discussion

The synthetic route to produce the nanostructured and porous hydrogel is shown in Scheme 3.1. Amphiphilic PCL-*b*-PEO-*b*-PCL block copolymers are synthesized, which form different microstructures in water depending upon the polymer concentration and the block lengths (a lamellar phase is shown as an example). The copolymers must be cross-linked prior to void formation in order to retain any spatial structure originating from the block copolymer templating. The ordered emulsion is cross-linked by electron beam, as the resulting cross-links do not degrade when the PCL blocks are removed through hydrolysis of their ester linkages. The terminal hydroxyl groups of PEO are restored when the PCL is removed, allowing later chemical modification.
In the following, each step is described.

3.3.1. Synthesis of PCL-*b*-PEO-*b*-PCL triblock copolymers and their microphase separation in water

PEO was reacted with ε-caprolactone in the presence of stannous octoate as a catalyst. Hydroxyl groups of PEO react with the catalyst, and this complex initiates the ring

opening polymerization of ε-caprolactone. Three different triblock copolymers were synthesized using different molecular weights of PEO macro-initiator, as shown in Table 3.1. Molecular weights and polydispersity indices of the synthesized triblock copolymers were determined by GPC, and block lengths of PCL were determined by ^{1}H-NMR. The triplet PCL peak at 4.067 *ppm* was compared with the singlet PEO peak at 3.651 *ppm* to determine the molecular weight of the PCL block (Cohn, 2002; Piao, 2003). The M_n of *Poly3* determined by GPC is lower than the M_n of the starting PEO homopolymer. This is perhaps due to degradation or may be related to the unusually high polydispersity and pronounced low-MW shoulder. Figure 3.1(a) shows the broad molecular weight distribution of *Poly3*, including an additional small peak at very low molecular weights that was not observed for *Poly1* and *Poly2*. The low-MW side peak suggests that *Poly3* contains degraded products of PEO or short PCL oligomers. The M_n reported in Table 3.1 was determined by considering the high molecular weight peak only. Comparing the GPC curves for the refractive index (RI) and UV detectors shows *Poly3* to contain a considerable amount of triblock copolymer rather than merely homopolymers, as is shown in Figure 3.1(b). Specific refractive index increments (*dn/dc*) of PEO and PCL in THF are comparable - 0.068 *ml/g* (Yuan, 1999) vs. 0.0795 *ml/g* (Knecht, 1972), respectively at 546 *nm*. Therefore, the RI intensity (measured at 690 *nm*) in Figure 3.1(b) indicates signals from both PEO and PCL, whereas the ultraviolet (UV) peak measured at 250 *nm* detects mainly PCL due to its ester groups (Campos, 2005). Although the RI and UV curves are not identical, their closely-located peak positions indicate *Poly3* chains are mostly block copolymer.

Microphase separation of PCL-*b*-PEO-*b*-PCL triblock copolymers in water was achieved by equilibrating aqueous solutions of the triblock copolymers at room temperature for one week, and the resulting microstructures were observed by SAXS. Figure 3.2 shows SAXS spectra of *Poly1* at various polymer concentrations. When *Poly1* was dissolved in water at a concentration of 20%, the emulsion sample has a peak at 40 *nm*. As polymer concentrations increase, *d*-spacing values of the emulsions decrease to 40, 34, and 29 *nm* at 40, 60, and 80% concentrations respectively. All SAXS peaks were analyzed as plots of Intensity*q^2 vs. q. Several peaks are recognized at high concentrations of 60% and 80%, and the q ratio between the three peaks is 1:2:3, indicating lamellar structure. The 80% emulsion

of *Poly2* shows a different q ratio, near $1:\sqrt{3}:\sqrt{4}:\sqrt{7}$, suggesting cylindrical structure (Figure 3.3). This will be further described in Chapter 5.

Scheme 3.1. Synthesis of nanostructured and porous hydrogel.

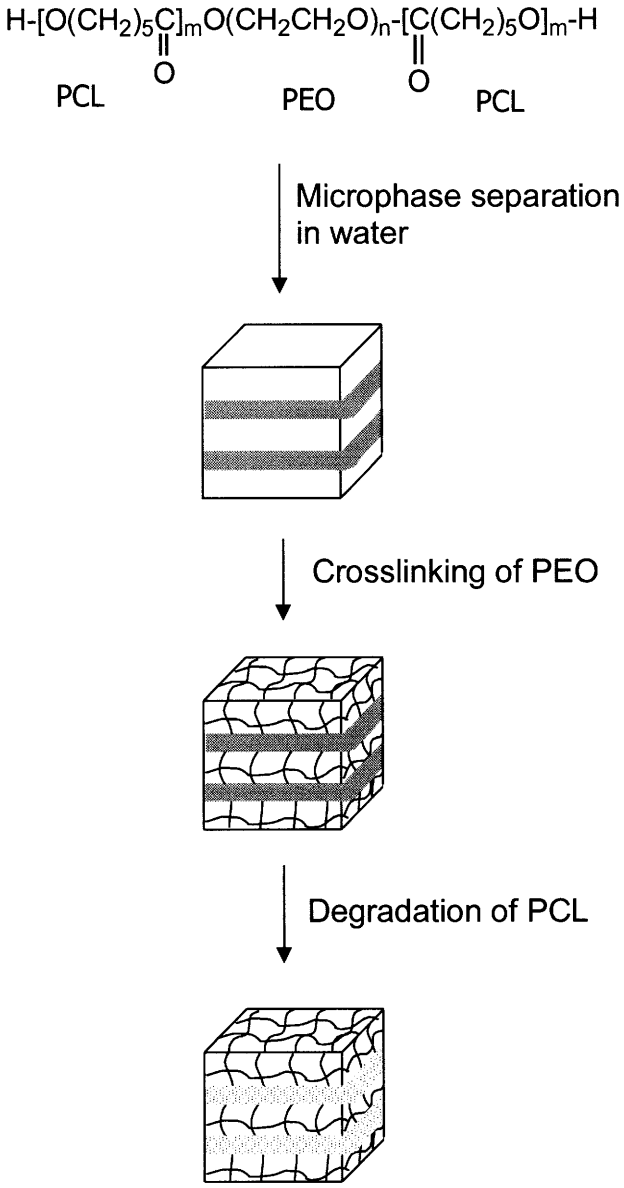

Table 3.1. PCL-*b*-PEO-*b*-PCL triblock copolymers synthesized.

	M_n (PEO)[a] *g/mol*	M_n (NMR)[b] *g/mol*	M_n[c] *g/mol*	M_w/M_n[c]	Polymerization yield (%)[d]
Poly1	15,000	7,500-15,000-7,500	29,000	1.23	58
Poly2	30,000	9,000-30,000-9,000	43,000	1.17	33
Poly3	47,000	19,000-47,000-19,000	36,000	2.55	46

[a] determined by GPC using starting PEO homopolymer; [b] determined by ^{1}H-NMR based on the M_n of PEO measured by GPC; [c] from GPC; [d] determined by comparing the amount of added ε-CL monomer and the M_n(NMR) of the PCL block.

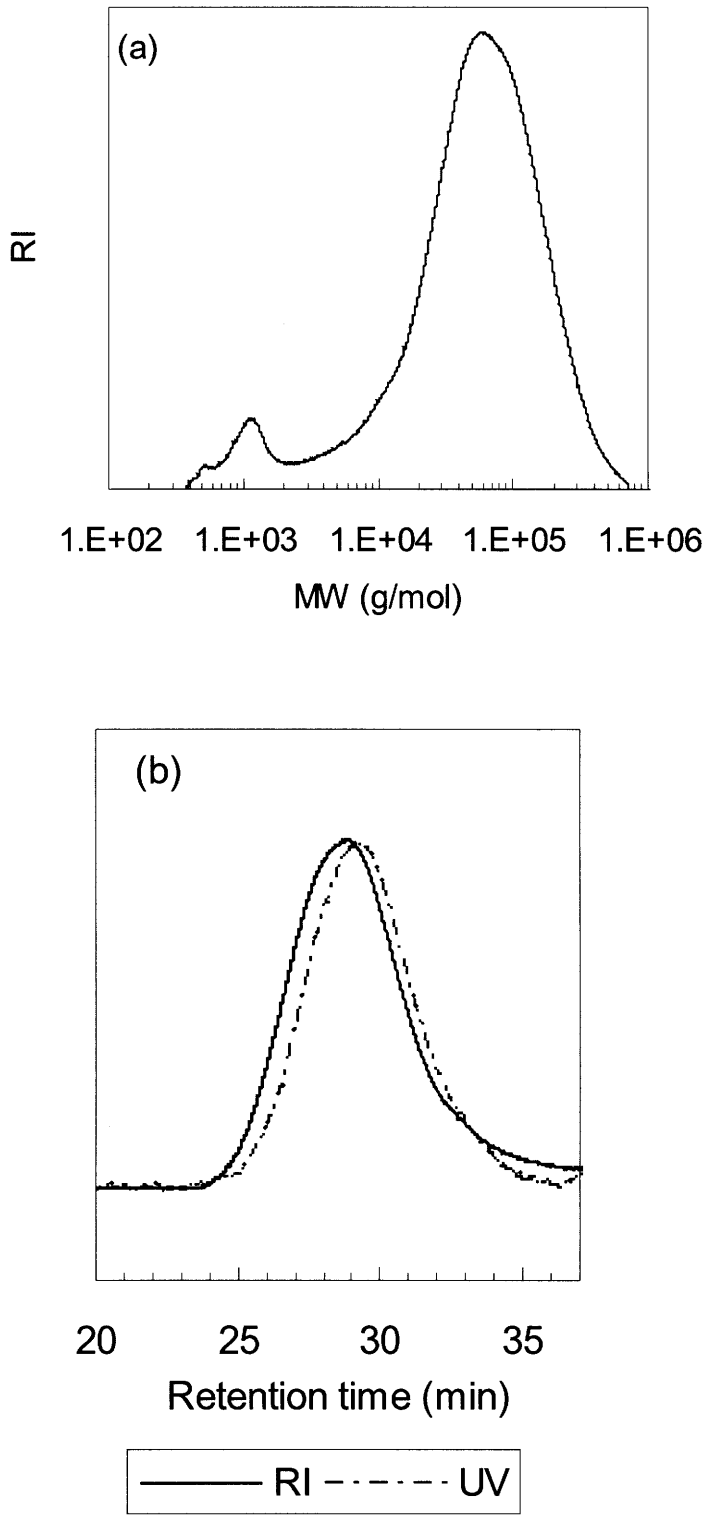

Figure 3.1. GPC of *Poly3*; (a) molecular weight distribution and (b) chromatogram.

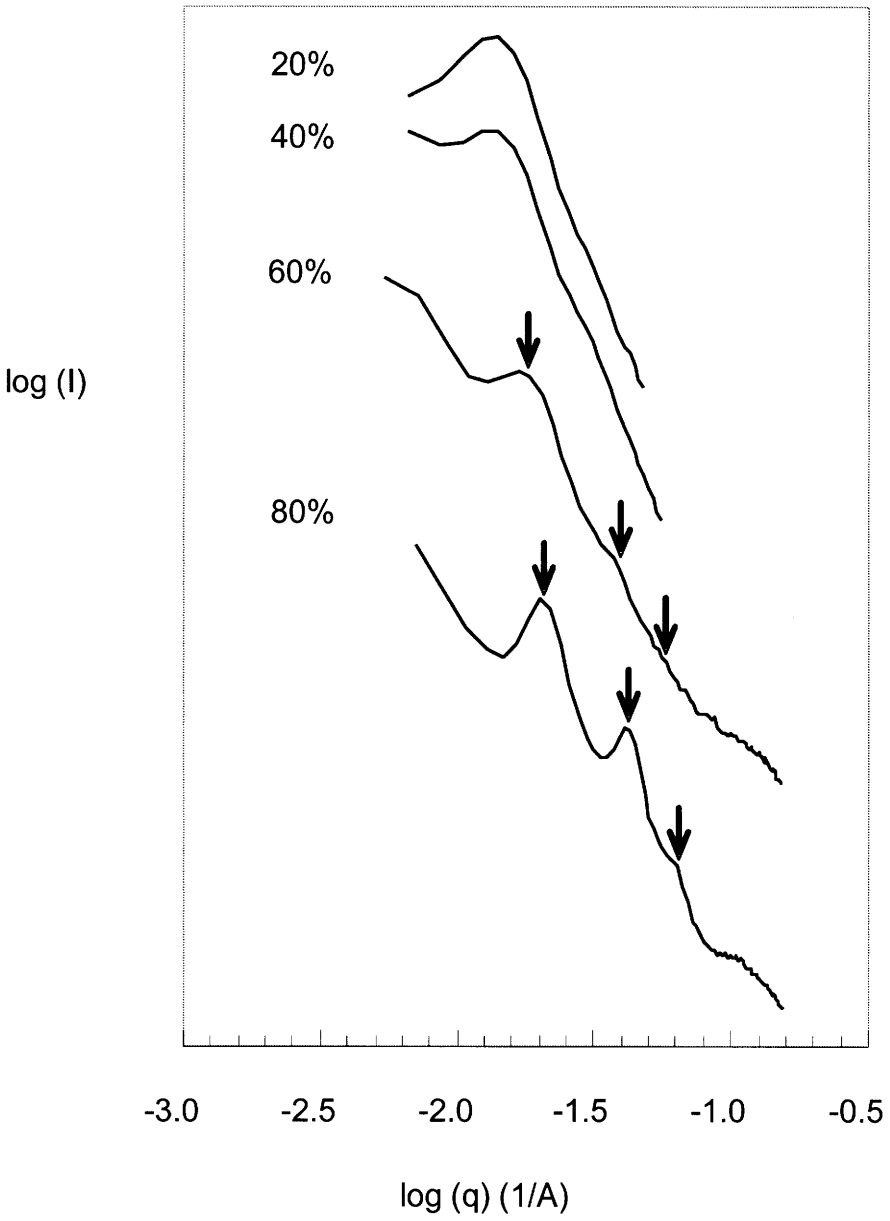

Figure 3.2. SAXS of *Poly1* at several concentrations in water; the arrows are expected peak positions for a lamellar microphase; the first order peaks for 20%, 40%, 60%, and 80% are 40 *nm*, 40 *nm*, 34 *nm*, and 29 *nm*, respectively.

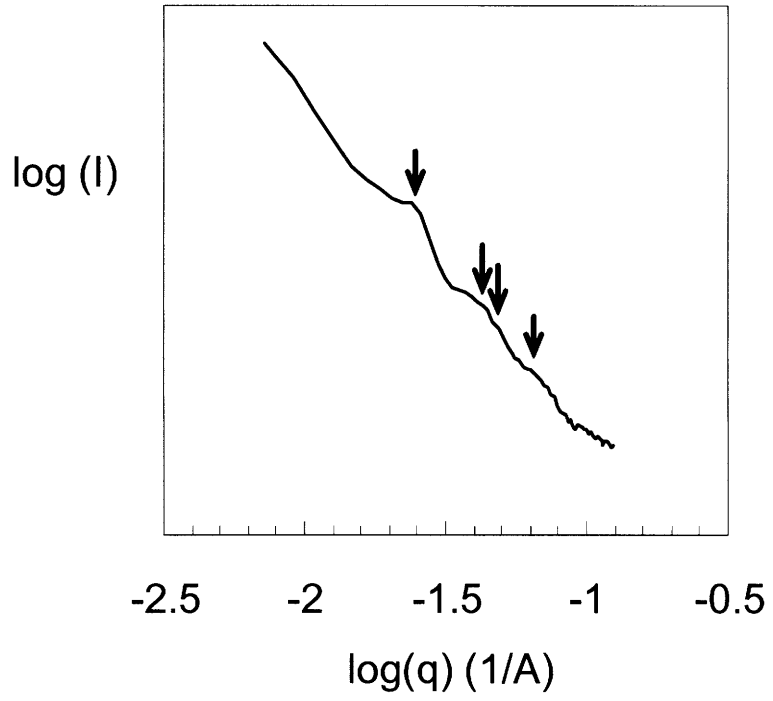

Figure 3.3. SAXS of *Poly2* at 80% in water; the arrows are expected peak positions for a cylindrical microphase; the first order peak was observed at 25 *nm*.

3.3.2. Cross-linking of PEO in PCL-*b*-PEO-*b*-PCL by electron beam irradiation

Cross-linking was performed by electron beam irradiation of aqueous solutions of PCL-*b*-PEO-*b*-PCL triblock copolymers. Under an electron beam, water is degraded to produce ·OH and O·⁻ radicals that abstract hydrogen from the -CH_2- groups of PEO. As cross-links are formed by the combination of these -·CH- radials, the presence of water accelerates cross-linking during irradiation (Dennison, 1986). The hydrophobic PCL is expected to be cross-linked less extensively as water plays such an important accelerative role. Gel fraction data after cross-linking show *Poly1* and *Poly3* to achieve near 100% gel fractions. In Figure 3.4, the gel fractions of the *Poly1* and *Poly3* that were synthesized in our lab are compared with that of a commercially-available diblock copolymer, PEO-*b*-PCL 5,000-4,000 *g/mol*. In the election beam cross-linking of PEO homopolymer (M_n = 15,000 *g/mol*), the molecular weight between cross-links (M_c) from swelling experiments was found to be dependent upon the polymer concentration; a M_c of 2,500 *g/mol* was obtained at 20% vs. values of ~4,000 *g/mol* at 40% and 60% concentrations. If it is assumed that a similar M_c is obtained in the block copolymers, it is understandable why the diblock copolymer, 5,000-4,000 *g/mol*, shows a lower gel fraction than the triblock copolymers with longer PEO blocks. At 40 and 60% polymer concentrations, a M_c of 4,000 *g/mol* means that there is on average only one cross-link in a PEO block of MW 5,000 *g/mol*. However, the numbers of cross-links per PEO block of weights 15,000 and 47,000 *g/mol* are sufficiently greater than one to yield high gel fractions even at high polymer concentrations. *Poly3* did not show a 100% gel fraction even though it has a long PEO block length, perhaps due to chain scission during electron beam irradiation.

Microstructures after cross-linking of the emulsions were observed by SAXS (Figure 3.5). Cross-linked samples were swollen in water, and SAXS measurements of these samples show that the micro-structures originating from microphase separation in emulsions were retained with slight increases in length scales. The effects of cross-linking upon the morphology of the amphiphilic networks were also investigated by AFM. Figure 3.6 presents an AFM phase image of *Poly1* cross-linked at 80% concentration for a dried sample. The image size is 1 μm x 1 μm, and the length scale of the observed structure is ~27 *nm*, while an

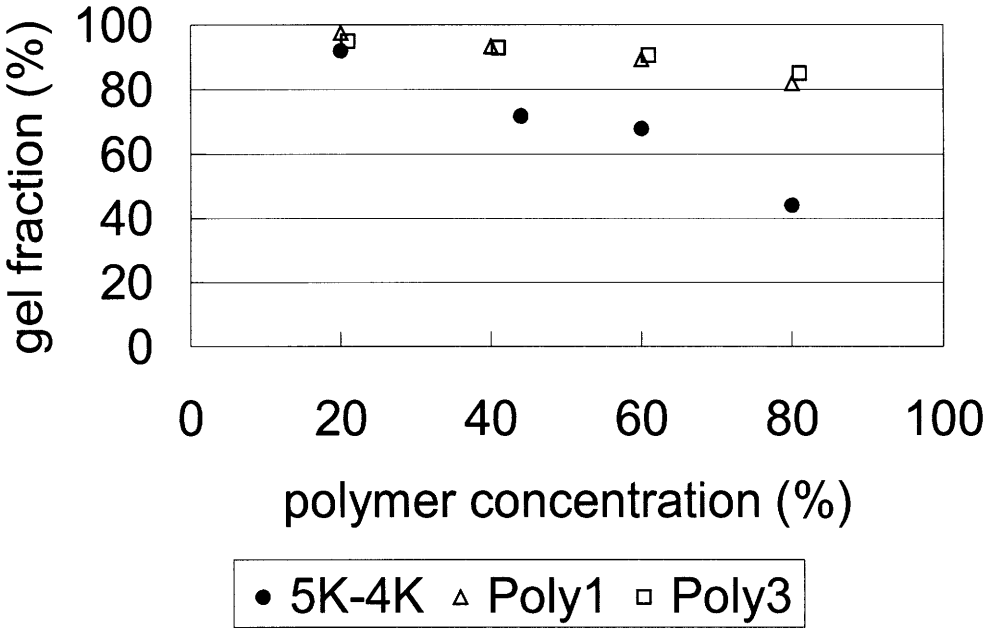

Figure 3.4. Gel fraction of block copolymers after electron beam cross-linking; 5K-4K denotes a commercially available PEO-*b*-PCL (M_n 5,000-4,000 *g/mol*).

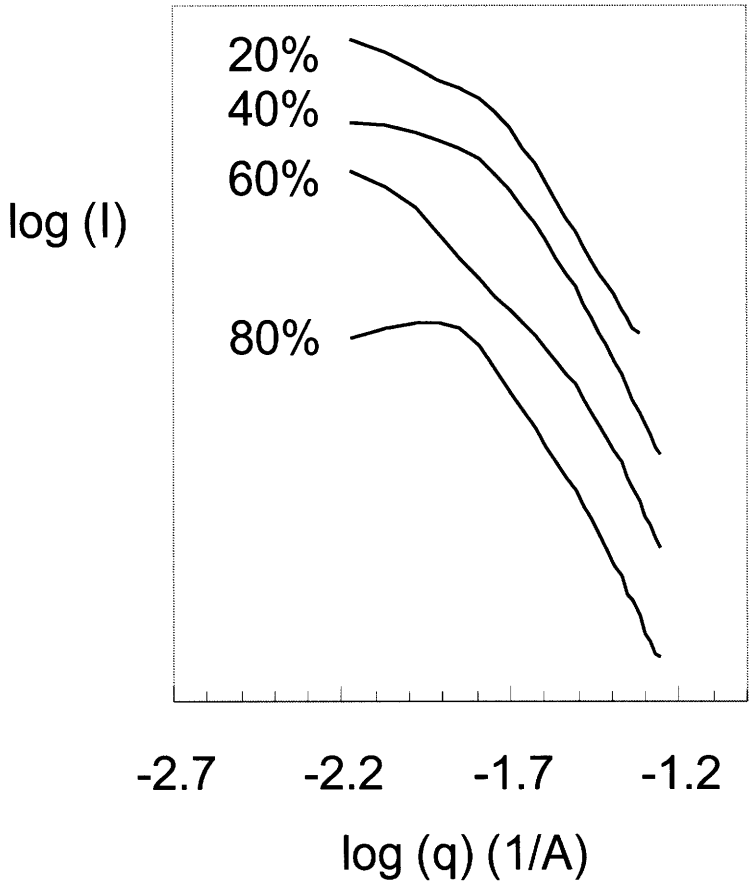

Figure 3.5. SAXS of *Poly1* after cross-linking in water; the first order peaks for 20%, 40%, and 80% are 35 *nm*, 37 *nm*, and 40 *nm*, respectively.

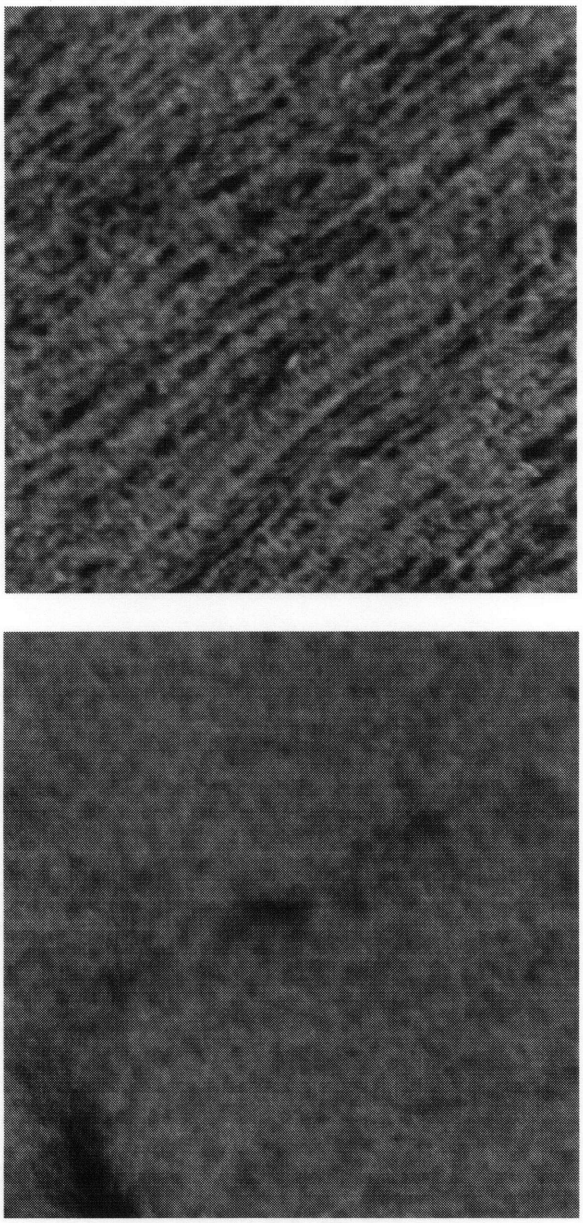

Figure 3.6. AFM phase images of the cross-linked polymers at 80% polymer concentration (dried sample); **top:** *Poly1* (lamellar structure, 27 *nm*); **bottom:** homopolymer PEO M_n=10,000 *g/mol*.

AFM image of a cross-linked homopolymer PEO shows no microstructure under similar conditions.

3.3.3. PCL degradation from cross-linked PCL-*b*-PEO-*b*-PCL

PCL was removed from the networks to produce nanostructured and porous PEO hydrogels. Ester linkages in the PCL blocks were degraded by hydrolysis in a NaOH*(aq)* solution, as shown in Scheme 3.2. The hydroxyl functional groups of PEO are restored following PCL removal.

FTIR was used to probe the absence of PCL in the degraded sample. As shown in Figure 3.7, the sample after the PCL degradation shows complete loss of the PCL-unique C=O peak at 1726 cm^{-1}. The weight loss after degradation of PCL supports this conclusion. As shown in Figure 3.8, *Poly3* is 44 % by weight PCL, and the measured weight losses of 46-51% suggest the complete removal of PCL with nearly complete retention of the PEO during degradation.

DSC results for *Poly1* in aqueous solution, after cross-linking, and after PCL degradation further confirm this picture of the synthesis process: microphase separation in water, PEO cross-linking, and PCL removal. As shown in Figure 3.9, some crystallinity of both the PEO and PCL blocks remain in aqueous "emulsions", which at higher polymer concentrations more resemble "pastes". The presence of two peaks indicates microphase separation. The lower of the peaks at 44°C is identified with PEO, in agreement with observed melting points in the presence of water for a homopolymer PEO sample, M_n=15,000 *g/mol*, with values of 50°C at polymer concentrations of 20, 40, 60, and 80% (Figure 3.9). The T_m of a PCL homopolymer, M_n=8,000 *g/mol*, was reported to be 55°C (Piao, 2003), and thus the second, higher peaks in the DSC curves at 53°C are identified with the PCL domains. Since crystallization of PEO is affected by the presence of PCL, the T_m of PEO is expected to decrease from the homopolymer value in triblock copolymers (An, 2001). As the polymer concentration is reduced, the lower, PEO peak becomes less intense, relative to the PCL peak, due to the increased local presence of water in the PEO domains. In addition, wet samples after cross-linking and PCL removal were studied by DSC as well

Scheme 3.2. Degradation of PCL in the PCL-PEO-PCL triblock copolymers.

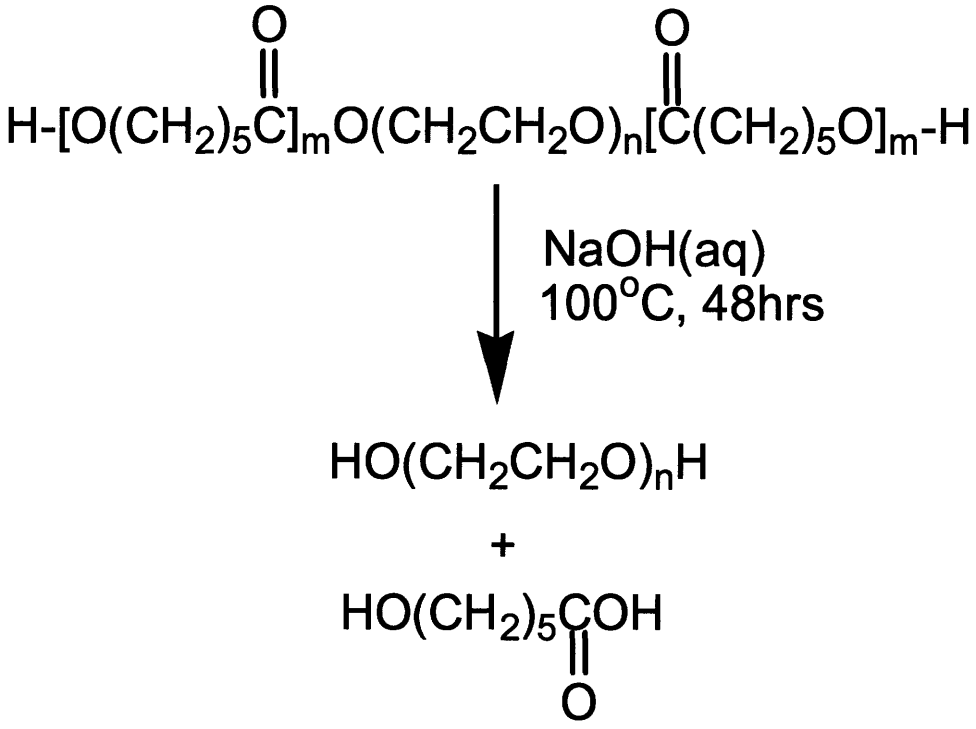

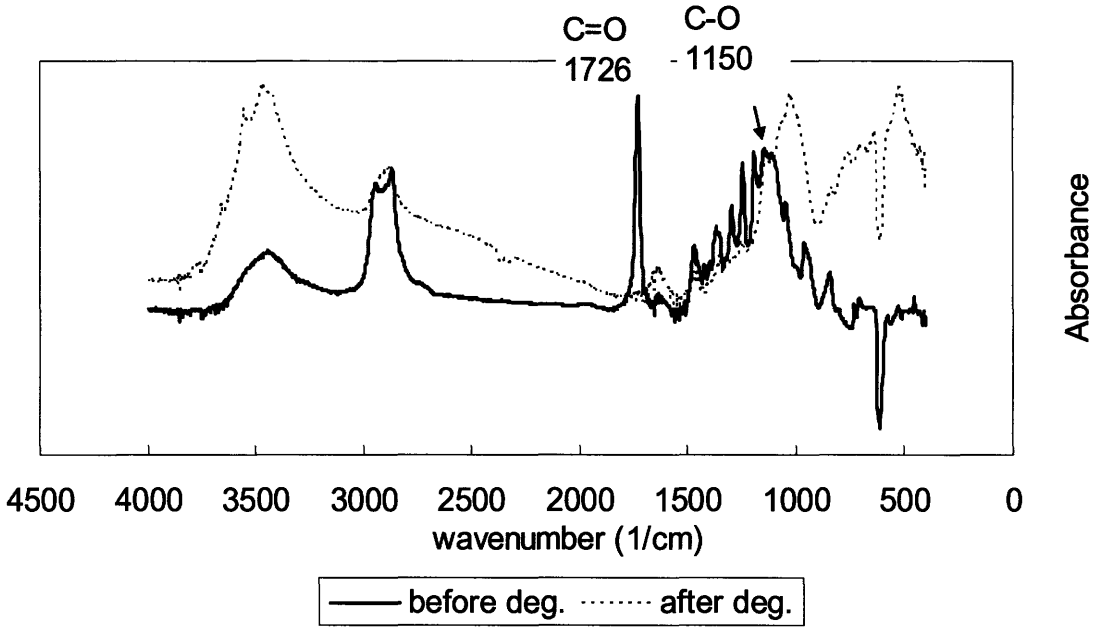

Figure 3.7. FTIR of *Poly3* before and after PCL removal.

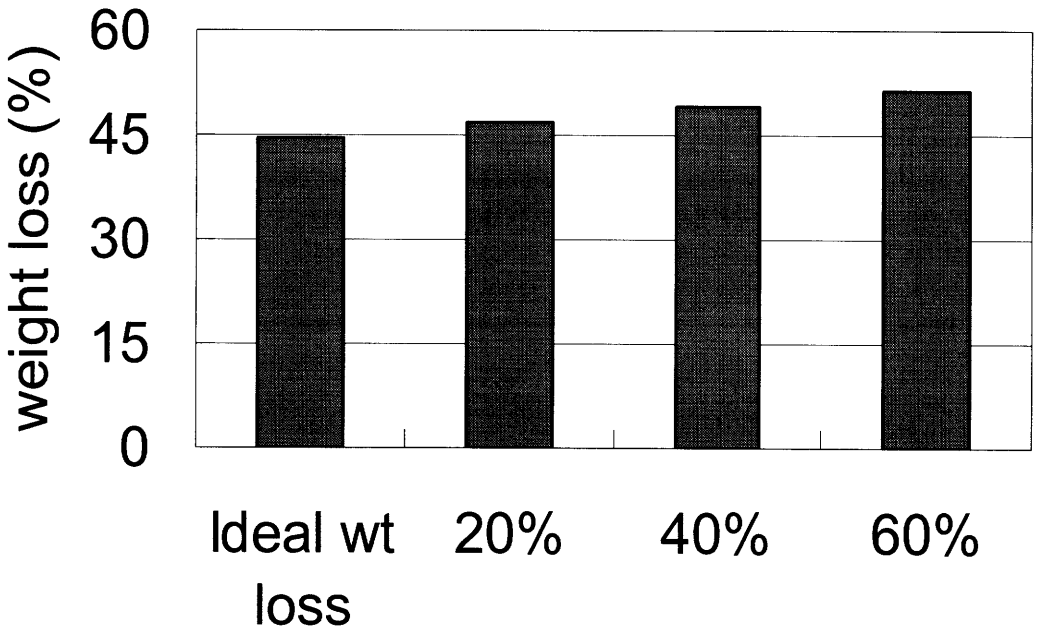

Figure 3.8. Weight loss after PCL degradation (*Poly3*); 20%, 40%, 60% denote samples that were cross-linked at 20%, 40%, 60% polymer concentrations followed by PCL removal.

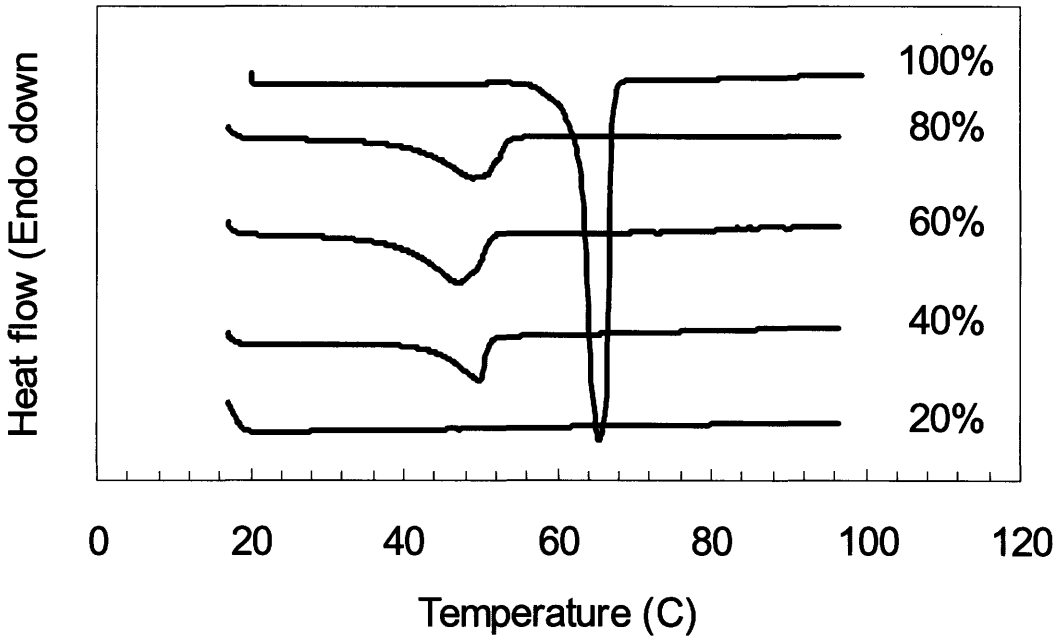

Figure 3.9. DSC of various aqueous solutions of PEO homopolymer (15 000g/mol); concentrations are polymer concentrations; aqueous solutions have T_m at ~50°C, while T_m of a 100% sample is 66°C.

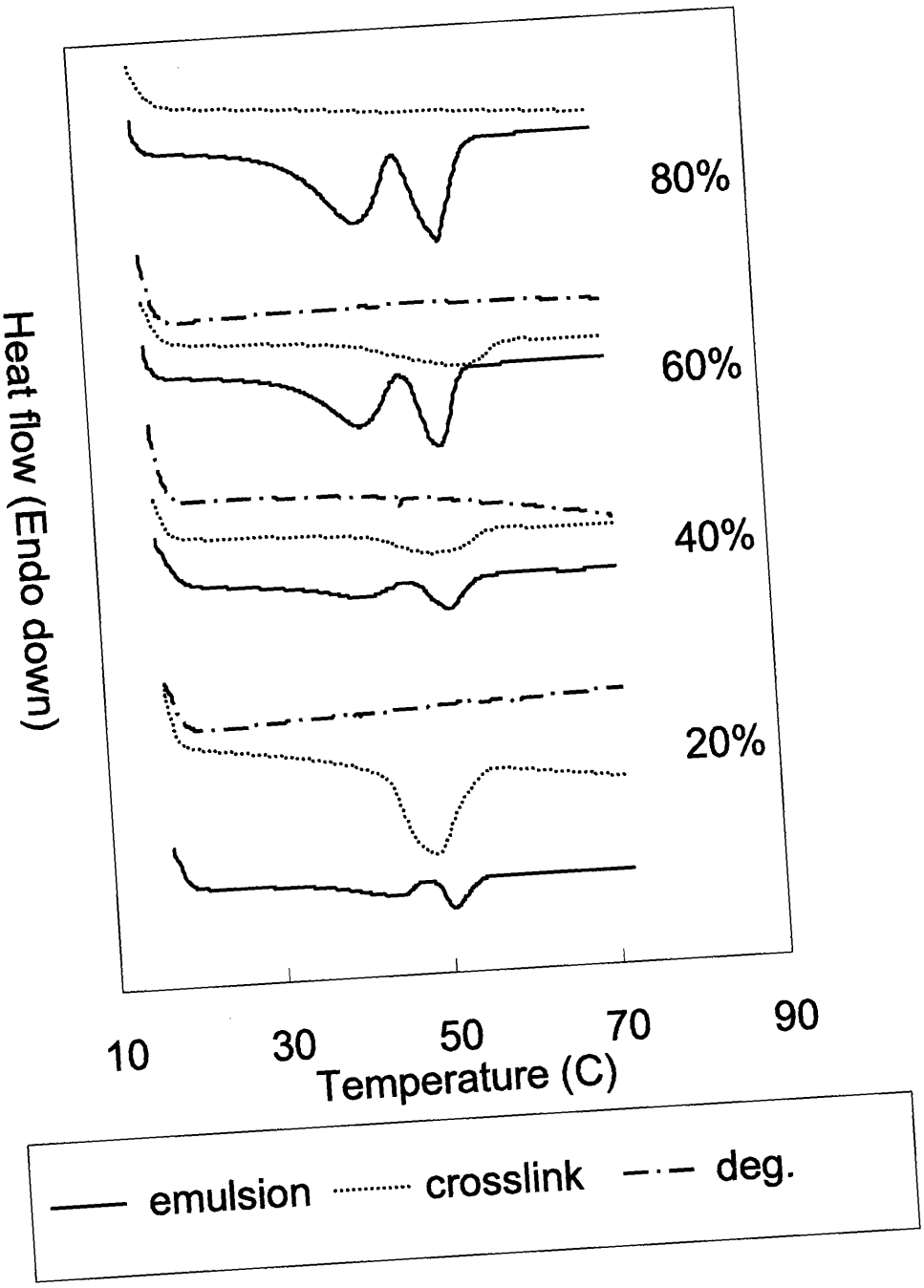

Figure 3.10. DSC of *Poly1* before and after cross-linking and after PCL degradation; in emulsion data, the first peak at around 44°C corresponds to the T_m of PEO, and the second at 53°C is that of PCL.

(Figure 3.10). Following cross-linking, the PEO peak is further reduced. Following degradation, the PCL peak is lost as well.

The nanostructured and porous PEO hydrogels were investigated with SAXS in the swollen state; however, no scattering peaks were observed following PCL removal. As this could occur if the length scales of the porous structures in the swollen hydrogels were beyond the detection limit of the SAXS apparatus, USAXS experiments were performed, but these as well showed no significant structure. Any "porous" hydrogel swollen in a good solvent (here water) has solvent everywhere, and the "pores" are defined as those regions in which there are no spanning polymer chains, which themselves constitute a minor component even in the "non-pore" regions. Thus, another possible explanation of the lack of observed structure in the SAXS spectra is a small contrast between "pores" and "matrix". SANS experiments in heavy water may provide greater contrast. Another explanation is that following PCL removal, the PEO further swells to reduce spatial heterogeneity. But even if this were the case, the resulting hydrogels yet may have interesting macromolecular transport properties due to the necessarily-inhomogeneous distribution of cross-links. There may exist "breathing modes" in which the hydrogel opens an O(10*nm*) void corresponding to the initial location of a PCL-rich domain, such that there are little or no PEO strands crossing the void to entangle a passing macromolecule. A study of transport properties is described in the next chapter.

3.3.4. Esterification of the nanostructured and porous PEO hydrogel

After PCL removal, the terminal hydroxyl groups of PEO are restored and become available for further chemical modification, providing new functional groups localized to the former domain boundaries. To confirm this, the porous PEO hydrogel produced by PCL degradation from *Poly3* was reacted with an excess of glutaric acid. The procedure is shown in Scheme 3.3. FTIR spectra of the reacted hydrogels following extraction show that ester groups are produced during this process. As shown in Figure 3.11, the presence of a C=O stretch at 1728 cm^{-1} and a hydrogen-bonded O-H stretch originating from carboxyl groups of the glutaric acid on the reacted hydrogel indicate that the hydroxyl groups at PEO termini are chemically available. For samples exposed to similar conditions but lacking the glutaric acid,

these signs of ester formation are not evident. If these hydroxyl groups are used to attach environmentally responsive materials, the pores may be further controlled by pH or temperature, which would be useful in biological applications such as drug delivery.

3.4. Conclusions

Nanostructured and porous PEO hydrogels were synthesized using amphiphilic PCL-*b*-PEO-*b*-PCL triblock copolymers. After microphase separation of the triblock copolymers in water, cross-linking of the PEO block was performed with an electron beam, followed by PCL removal through hydrolysis. Microphase structures were observed by SAXS (emulsion samples) and AFM (cross-linked samples); mostly lamella yet cylindrical in one instance. SAXS experiments following PCL removal showed no significant structure, perhaps due to a lack of contrast in swollen states of the "porous" hydrogels. To further investigate these materials, macromolecular transport experiments were performed and described in the following chapter. These nanostructured and porous hydrogels have hydroxyl functional groups available for further chemical modification and can be used in biomedical or pharmaceutical applications.

Scheme 3.3. Esterification of the nanostructured and porous hydrogel with glutaric acid.

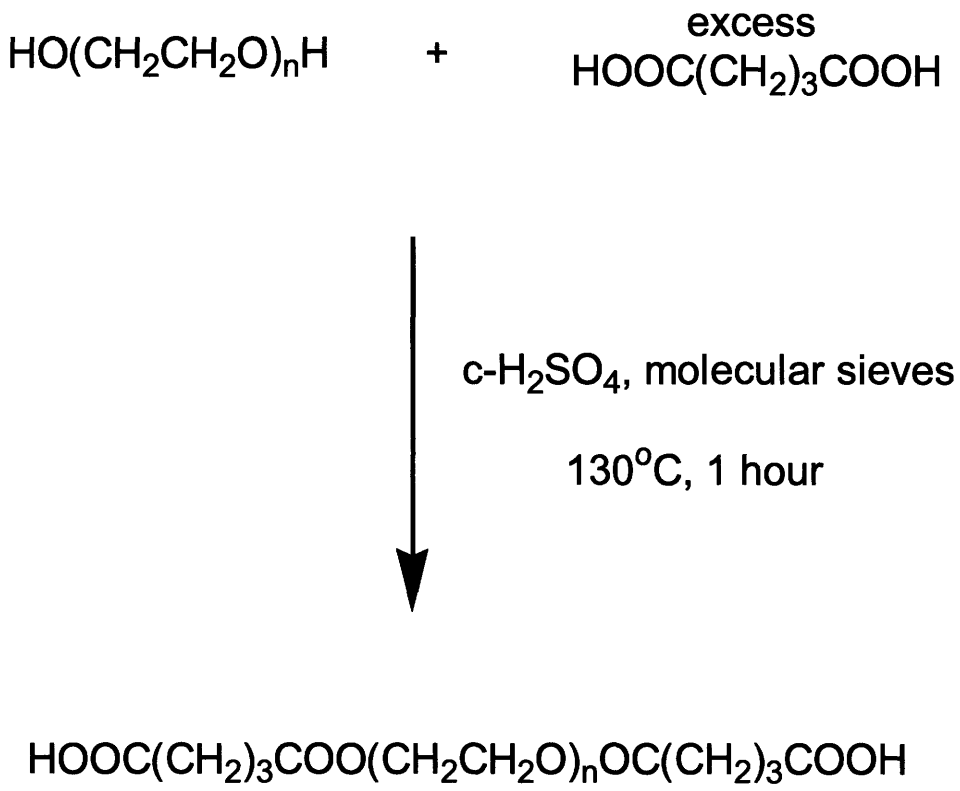

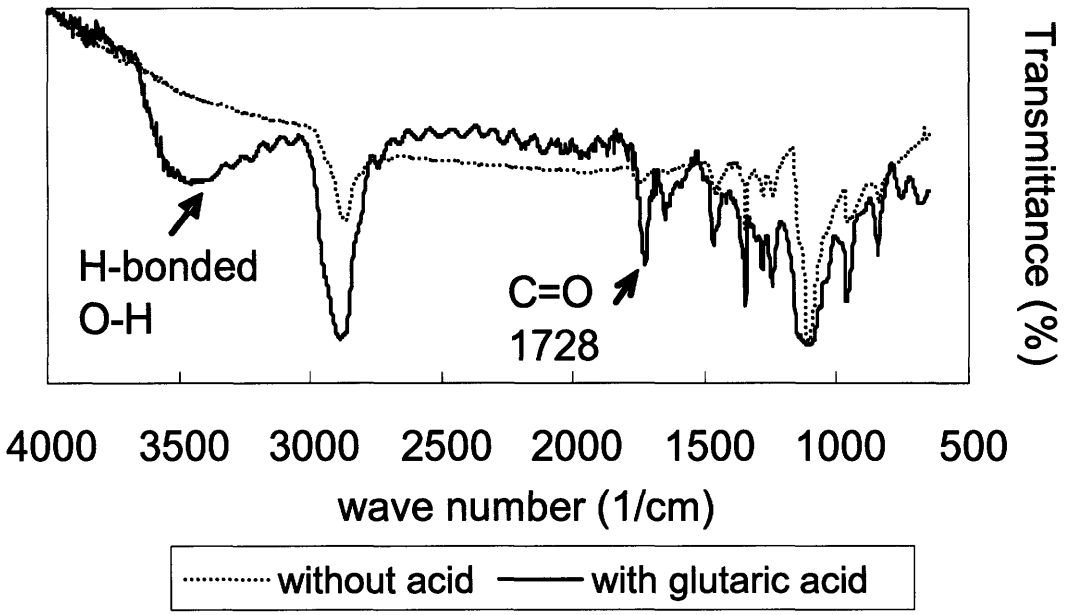

Figure 3.11. FTIR of the nanostructured and porous PEO hydrogels after treatment in esterification reaction conditions with (*solid line*) and without (*dotted line*) glutaric acid.

4. Macromolecular Transport through Nanostructured and Porous Hydrogels Synthesized Using the Amphiphilic Copolymer, PCL-*b*-PEO-*b*-PCL

4.1 Introduction

Amphiphilic block copolymers have been studied extensively due to their interesting combination of hydrophilic and hydrophobic behavior. In particular, poly(ethylene oxide)/poly(ε-caprolactone) (PEO/PCL) block copolymers are widely used in drug delivery systems because of their biocompatibility and biodegradability (Gan, 1999; Yoo, 1999; Zhao, 1999; Park, 2002; Ge, 2002; Nie, 2003).

Hydrogels are produced by crosslinking hydrophilic polymers such as PEO, and the mesh size determined by crosslink density governs the mobility of penetrant molecules. Molecules smaller than the mesh size pass relatively easily through the gel while larger particles become entangled with the polymer chains of the network and diffuse more slowly. The mesh size is the characteristic size of the "voids" in the swollen gel that are filled with fluid and have no spanning polymer chains.

Diffusion through gels has been studied for fluorescent molecules and particles using the technique of Fluorescence Recovery after Photobleaching (FRAP) (Kosto, 2004; Cheng, 2002; De Smedt, 1997). Kosto and Deen (2004) studied the diffusion of fluorescein-labeled proteins and polysaccharide through agarose and agarose-dextran composite gels. Cheng and Prud'homme have examined the effect of crosslink density on transport through PEO gels (Cheng, 2002), establishing a clear relationship between penetrant size and the mesh size of the matrix. When the penetrant is comparable to the mesh size, the diffusivity through the hydrogel is much lower than that observed in water, yet for very small penetrants the hydrogel and water diffusivities are comparable in magnitude.

This work presents FRAP data for macromolecular transport through nanostructured and porous hydrogels synthesized using PCL-*b*-PEO-*b*-PCL block copolymer templating. Microphase-separated emulsions of the block copolymer in water are crosslinked in an electron beam to obtain hydrogels with similar spatial structure as the emulsions. The PCL domains then are removed through hydrolysis to form porous PEO hydrogels (Kang, 2006). Even if the mesh size in the crosslinked PEO domains were small, the regions formerly

occupied by the PCL domains have no spanning PEO chains and should introduce new channels for macromolecular transport. As well, the porous PEO hydrogels have functional groups near the pore regions that are available for further chemical modification (Kang, 2006). These materials potentially offer high macromolecular diffusivities with the possibility of chemical modification, and so show promise for use in drug delivery and separation.

4.2. Experimental Section

4.2.1 Materials

PEO 45 *kg/mol*, ε-caprolactone, stannous octoate, and a dye (Acid yellow 73) were purchased from Sigma-Aldrich and used without further purification. Sodium azide and methanol were purchased from Mallinckrodt (Phillipsburg, NJ) and the solvents (dichloromethane, *n*-hexane) were obtained from EMD Chemicals (Gibbstown, NJ). Fluorescein-conjugated proteins (parvalbumin 12 *kDa*, and BSA 68 *kDa*) and carboxylated polystyrene beads (nominal diameter 20 *nm*) were purchased from Molecular Probes Inc. (Eugene, OR). Capillary tubes (300 μm in thickness) were obtained from VitroCom Inc. (Mountain Lakes, NJ).

4.2.2 Synthesis of PCL-b-PEO-b-PCL triblock copolymers

10 *g* of PEO (45 *kg/mol*) was dissolved in 30 *ml* of toluene, and the mixture was heated to 130°*C* in a nitrogen atmosphere to evaporate the solvent and any water that might have been in the PEO. A mixture of 10 *ml* of ε-caprolactone and three drops of stannous octoate as a catalyst was added and the resulting reaction medium was held at 130°*C* for 21 hours under a nitrogen atmosphere. The synthesized block copolymer was purified with dichloromethane and cold *n*-hexane three times. The final product was dried in a hood at room temperature for one day and in a vacuum oven at 40°*C* for another two days. The polymerization yield was 42 %.

4.2.3. Crosslinking of PCL-b-PEO-b-PCL by electron beam irradiation

PCL-*b*-PEG-*b*-PCL in a 5 *cm* dia. Petri dish was heated to 70°*C* for one day, and after cooling to room temperature, Milli-Q water with 0.01% NaN_3 was added to make an emulsion of the desired concentration. After equilibration at room temperature for more than two days, the aqueous solution was crosslinked by an electron beam to form a hydrogel (Kang, 2006). The temperature during irradiation was controlled below 50 °*C* through use of a slow dose rate and a fan. For an emulsion at a 20 % polymer concentration, a 30 *Mrad* dose was administered, with 50 *Mrad* doses being used at 40%, 60%, and 80% polymer concentrations. After extraction with 0.01% NaN_3 Milli-Q water, the crosslinked samples were dried in a vacuum oven at 40°*C* for two days.

A PEO homopolymer (45 *kg/mol*) was also crosslinked under the same conditions to serve as a control. An average molecular weight between crosslinks (M_c) of the PEO hydrogel was calculated from swelling experiments in water using the following equation,

$$\frac{1}{M_c} = \frac{2}{M_n} - \frac{\ln(1-v_{2s}) + v_{2s} + \chi_{FH} v_{2s}^2}{V_1 \rho_2 v_{2s}^{1/3} - v_{2s}/2} \qquad (1)$$

M_n is number average primary polymer molecular weight, v_{2s} is polymer volume fraction at equilibrium swelling, V_1 is molar volume of solvent, ρ_2 is polymer density, and χ_{FH} is Flory-Huggins interaction parameter (0.426 between water and PEO at room temperature as determined by osmometry; Dennison, 1986). The mesh size of the hydrogel was calculated using the swelling ratio and the M_c as follows (Cananl, 1989).

$$\xi = Q^{1/3} \left(\overline{r_0^2}\right)^{1/2} \qquad (2)$$

ξ is the mesh size, Q is the equilibrium volume ratio of the swollen and unswollen polymers, and $\left(\overline{r_0^2}\right)^{1/2}$ is unperturbed root-mean-square end-to-end distance between crosslinks. $\left(\overline{r_0^2}\right)^{1/2}$ for PEO was calculated using the following equation,

$$\overline{r_0^2} = \frac{3 M_c C_\infty l^2}{M_0} \qquad (3)$$

M_0 is the molecular weight of a repeat unit, C_∞ is the characteristic ratio (3.88 for PEO [13]), and l is an average bond length (1.46 Å for PEO; Sundararajan, 1996).

4.2.4. Degradation of PCL in the crosslinked sample

Ester linkages of PCL were hydrolyzed in 0.5*M* NaOH in 40/60 (*v/v* %) methanol/water solutions, and the product was extracted with 40/60 (*v/v* %) methanol/water solutions and pure water. The final products were dried in a vacuum oven at 40°*C* for two days.

4.2.5. Transport properties of the nanostructured and porous hydrogel

The transport properties of the resulting nanostructured and porous hydrogel following PCL removal were then studied. A dry sample of the gel was embedded in LR white resin, and after drying for one day, was microtomed to produce a thin film (thickness 100~150 *μm*). These films were swollen in fluorescein or fluorescein-labelled macromolecules (parvalbumin 12 *kDa*, BSA 68 *kDa*, and carboxylated polystyrene beads-nominal diameter 20 *nm*) solutions that were prepared with a buffer of PBS, pH 7.4. The swollen films were mounted on a microslide and were enclosed by a cover glass. Silicon sealant was used to prevent evaporation. Diffusion coefficients of various penetrants were measured by Fluorescence Recovery After Photobleaching (FRAP), as described in detail in ref. 7. A photobleaching spot was generated by a strong laser beam, and the shrinking of the spot with time was observed. From the time scale of the recovery process and the initial physical size of the spot, the diffusivity of the fluorescein (or fluorescein-labeled) molecule can be estimated. As a control, diffusion coefficients were also measured in a PEO gel synthesized from PEO homopolymer (45 *kg/mol*) under similar conditions. Thus a comparison of the nanostructured hydogel to the control shows directly the effect upon transport properties of the nanoscale porosity. The diffusion coefficient in water (D_∞) of each penetrant was measured in a capillary tube (300 *μm* in thickness). D_∞ was used to calculate each penetrant's Stokes-Einstein radius (r_s) (Kosto, 2004),

$$r_s = \frac{k_b T}{6\pi \mu D_\infty} \qquad (4)$$

k_B is Boltzmann's constant, T is the absolute temperature, and μ is the viscosity of a solution.

4.2.6. Characterization

Number and weight average molecular weights (M_n and M_w respectively) and polydispersities (M_w/M_n) were obtained with a Waters Gel Permeation Chromatograph (GPC) at the University of Akron using tetrahydrofuran (THF) as the solvent at a 1 *ml/min* elution rate with calibration through use of polystyrene standards. Proton Nuclear Magnetic Resonance (^{1}H-NMR) spectra were acquired by a 300 *MHz* Varian Mercury apparatus using $CDCl_3$ as a solvent at the MIT Department of Chemistry Instrumentation Facility (DCIF). Small Angle X-ray Scattering (SAXS) experiments were performed at the Institute for Soldier Nanotechnologies (ISN) at MIT. Aqueous emulsions of triblock copolymers were enclosed in Kapton™ tape. SAXS data were collected for exposures of 1,000 *sec* at room temperature. Background calibration was performed by subtracting the signals from the corresponding empty Kapton™ tape holders. Atomic Force Microscopy (AFM) images were taken with a Veeco Metrology Group Nanoscope IV Scanning Probe Microscope (Digital Instruments) at the MIT Center for Material Science and Engineering (CMSE). Dry samples were microtomed to produce smooth surfaces for AFM measurement. Fourier Transform Infrared Spectroscopy (FTIR) measurements were conducted using a Nicolet Magna 860 at CMSE. Samples for IR measurement were vacuum-dried at 40°*C* for at least two days prior to analysis and prepared by crushing a dry sample to form a thin film on a NaCl sample window.

4.3. Results and Discussion

4.3.1. Synthesis of high molecular weight of PCL-b-PEO-b-PCL

A high molecular weight of poly (ε-caprolactone-*b*-ethylene oxide-*b*-ε-caprolactone) (PCL-*b*-PEO-*b*-PCL) triblock copolymer was synthesized by ring opening polymerization of ε-caprolactone with PEO (45 *kg/mol*) as a macro-initiator in the presence of stannous octoate as a catalyst. High molecular weight polymers are favored as they improve the mechanical strength and gel fraction of the hydrogels following electron beam crosslinking (Kang, 2006). Table 4.1 shows the molecular weights of the triblock copolymer, E45CL30, as determined

Table 4.1. PCL-*b*-PEG-*b*-PCL triblock copolymer synthesized.

	M_n (PEO)[a] *g/mol*	M_n (NMR)[b] *g/mol*	M_n[c] *g/mol*	M_w/M_n[c]
E45CL30	45,000	10,000-45,000-10,000	51,000	1.27

[a] determined by GPC using starting PEO macro-initiator; [b] determined by ^{1}H-NMR based on the M_n of PEO measured by GPC; [c] from GPC

by ^{1}H-NMR and GPC. It has 30% of PCL as determined by ^{1}H-NMR (Figure 4.1). There is a distinctive PEO peak at 3.651 *ppm*, which was compared with the PCL peak at 4.067 *ppm* to estimate the block ratio of PEO to PCL. GPC was also used to determine the molecular weight and polydispersity of the triblock copolymer. As shown in Figure 4.2, the triblock copolymer exhibits an increase in molecular weight and slightly a broader molecular weight distribution following polymerization from the PEO macro-initiator.

4.3.2. Microstructures of E45CL30

The morphology of E45CL30 in water was studied using SAXS. For this, the triblock copolymer was annealed at 70^oC (above the melting points of both PEO and PCL) for one day, and after cooling to room temperature, water was added to produce emulsions of the desired concentrations. These were equilibrated at room temperature for two days before SAXS measurement. As shown in Figure 4.3, high concentration samples show more pronounced peaks. At 100%, the q ratios of the three peaks are 1:2:3, indicating lamellar morphology. The shorter block length of PCL than that of PEO tends to produce cylindrical morphology, as seen in the sample prepared at room temperature without heating (in more detail in Chapter 5). However, when it is heated above melting point of both blocks, and recrystallized at room temperature, as done here, lamellar morphology is observed. As the polymer concentration decreases, the SAXS peaks weaken.

The morphology formed at an 80 % polymer concentration was fixed by electron beam crosslinking. The morphology of a dried sample of the resulting hydrogel was investigated by AFM. Figure 4.4 shows a 500 *nm* x 500 *nm* phase image that exhibits a lamellar morphology with a 20 *nm* spacing. This is in good agreement with SAXS, considering the loss in water that occurs when drying the gel.

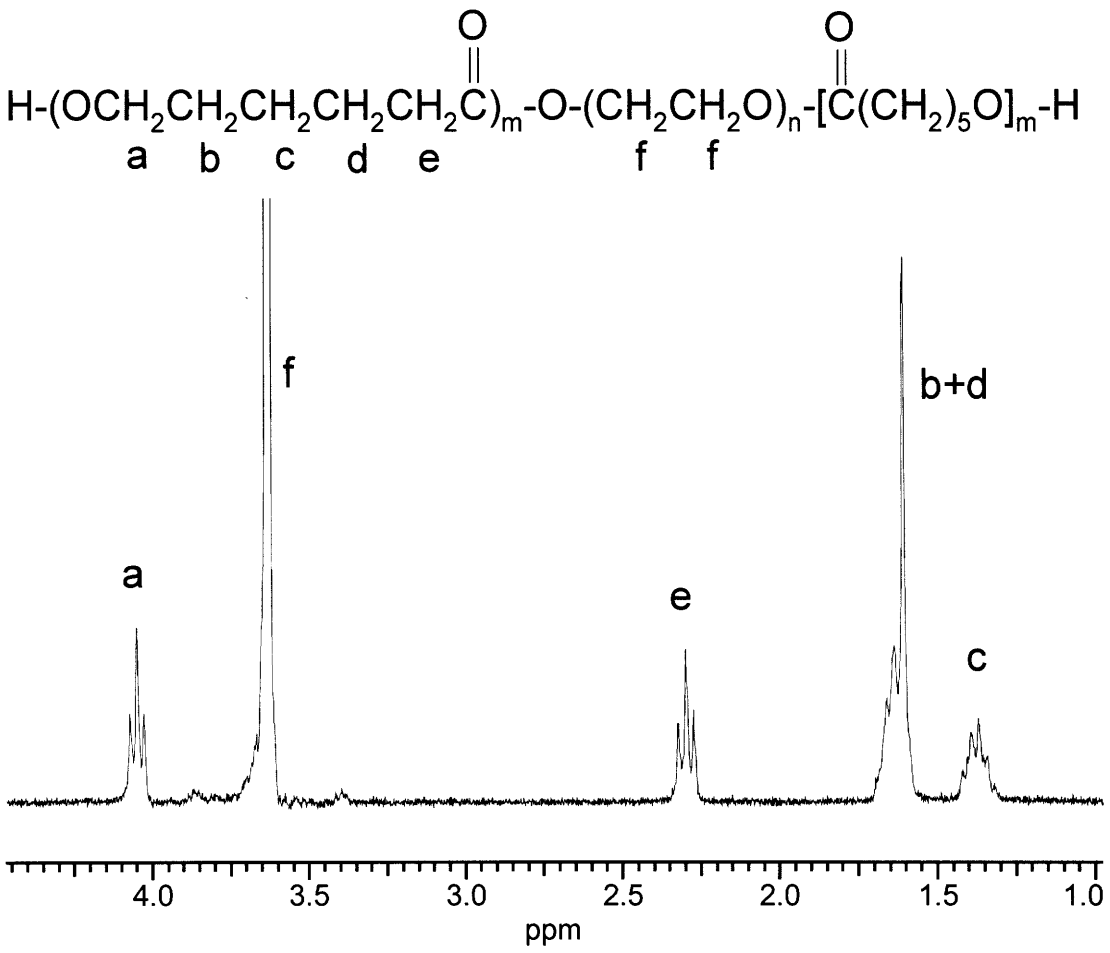

Figure 4.1. ^{1}H-NMR of E45CL30.

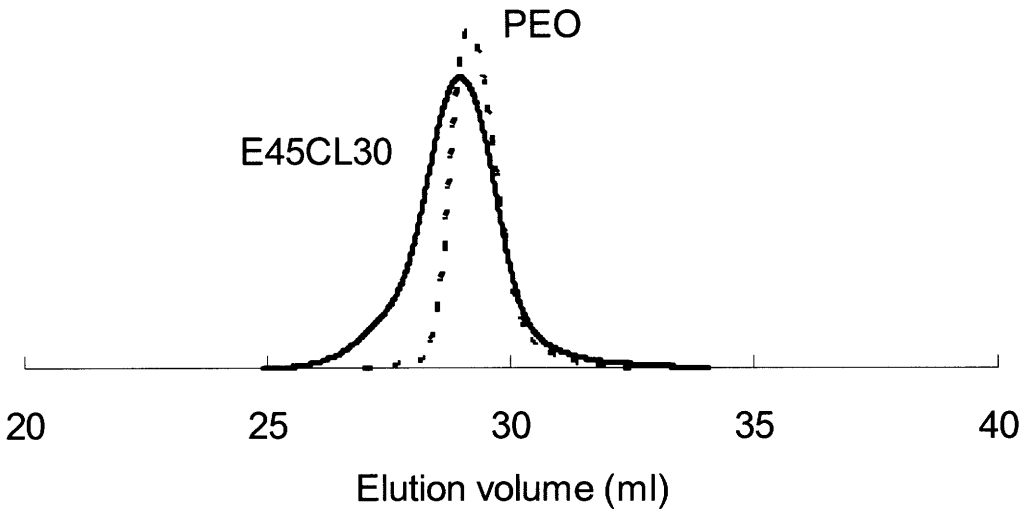

Figure 4.2. GPC of the PEO macro-initiator and E45CL30.

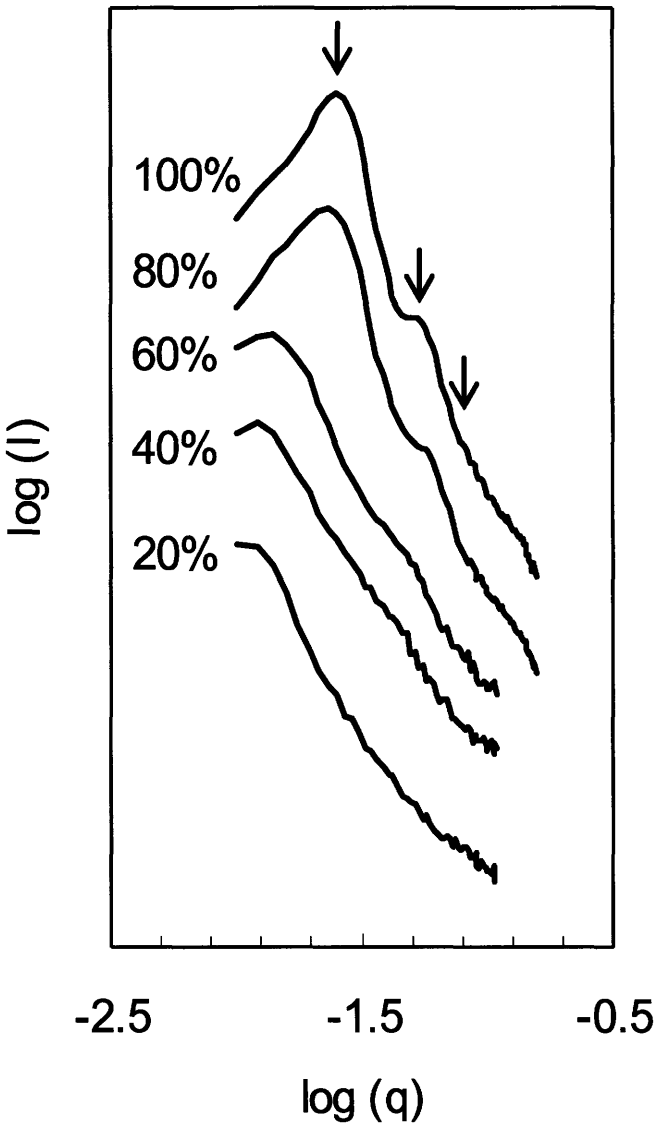

Figure 4.3. SAXS of aqueous solutions of E45CL30. The arrows are the expected peak positions for a lamellar microphase. The first order peaks for concentrations of 40%, 60%, 80%, and 100% are 52 *nm*, 45 *nm*, 26 *nm*, and 25 *nm* respectively.

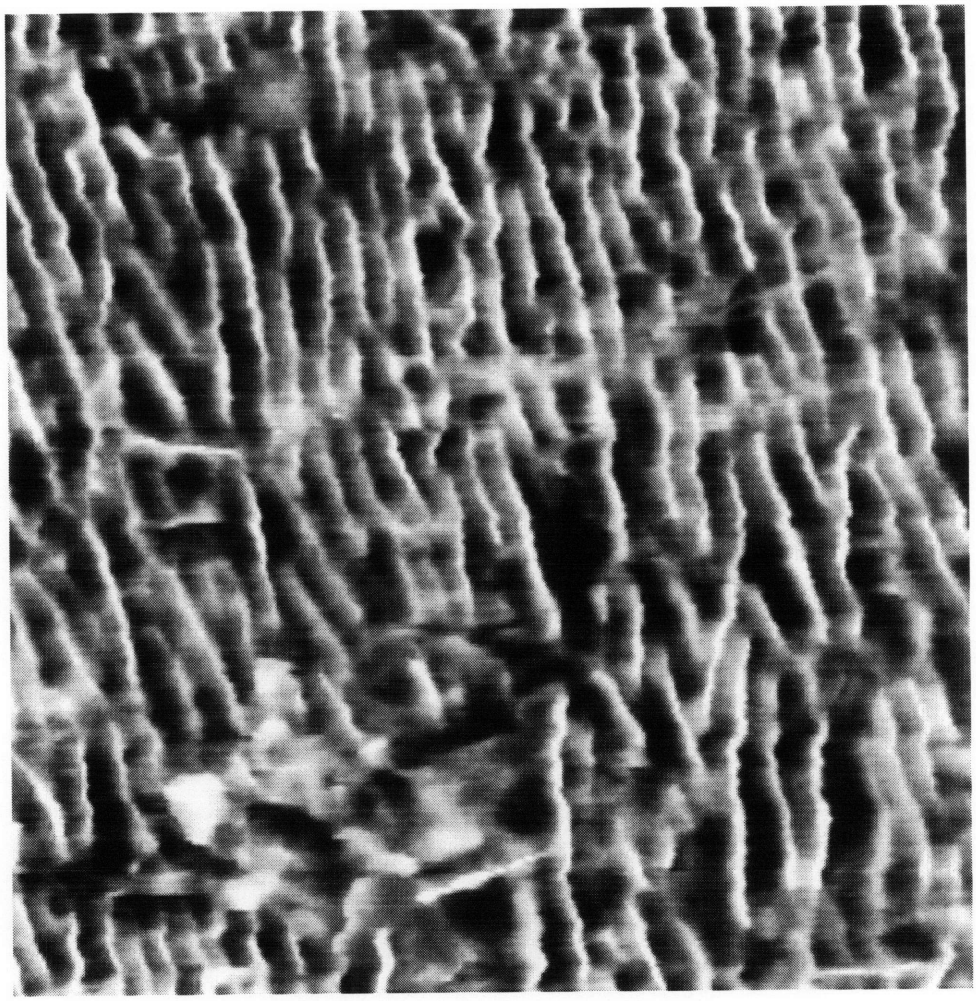

Figure 4.4. An AFM phase image of E45CL30 after crosslinking at 80% polymer concentration (dry sample, 500 *nm* scan size). It has a lamellar structure (20 *nm*).

4.3.3. Synthesis of nanostructured and porous hydrogel

Next, the PCL segments were removed in the crosslinked samples by hydrolysis of their ester linkages. PCL removal was confirmed by FTIR as shown in Figure 4.5. Disappearance of the C=O peak at 1726 cm^{-1} suggests that PCL was completely degraded and removed.

4.3.4. Transport properties

The nanostructured and porous hydrogel is expected to have porous openings produced by PCL removal in addition to the mesh regions between chain crosslinks found in a homogeneous gel. Because of this additional porosity, the nanostructured and porous hydrogel swells more upon addition of water (a twelve-fold increase in volume over the dry state) than the homogenous control gel obtained from the same PEO homopolymer under the same conditions (which exhibits only a six-fold increase in volume). To further investigate this structural difference, diffusion coefficients of various penetrants were measured in this nanostructured and porous hydrogel and the control PEO homopolymer network. The mesh size of the PEO network is ~12 *nm*, which was determined by swelling experiments in water. Table 4.2 shows the various penetrant molecules used and their Stokes-Einstein radii (r_s) calculated from the diffusivity in water (D_∞) determined by FRAP experiments.

Due to the presence of pores produced by PCL removal, the nanoporous hydrogel is expected to have higher diffusion coefficients than the homogeneous control PEO homopolymer gel. This behavior is indeed observed in Figure 4.6, which plots the reduced diffusion coefficients (diffusion coefficient in the hydrogel divided by D_∞) in the two gels for various penetrants. Over a range of penetrant sizes, penetrant diffusion is indeed faster in the nanostructured hydrogel than in the homogeneous control gel. Furthermore, a penetrant of size ~8 *nm* did not exhibit sufficient fluorescent intensity in the homogeneous control PEO gel for FRAP measurement, suggesting that the penetrant was unable to diffuse into the hydrogel within a reasonable time frame. However, its diffusion coefficient in the nanostructured and porous hydrogel remained relatively high.

To investigate further, an additional homogeneous PEO gel with a larger mesh size (~36 *nm*) was synthesized by using a smaller electron beam dose. The ~8 *nm* penetrant was able to diffuse into this looser network and exhibited a high diffusivity. For all gels, the polystyrene bead (~27 *nm* in diameter) was too large to enter and have its diffusivity measured by FRAP. The data of Figure 4.6 show that the nanostructured hydrogels have the high macromolecular transport rates of a much looser network, while retaining the high crosslink density in the PEO domains.

4.4. Conclusion

A nanostructured and porous hydrogel was synthesized using PCL-*b*-PEO-*b*-PCL block copolymer templating. An emulsion of the block copolymer in water was crosslinked in an electron beam and exhibited lamellar morphology. The PCL domains were then removed through hydrolysis. The regions formerly occupied by PCL offer additional channels for macromolecular transport through the gel. A hydrogel with this nanostructured porosity was found through FRAP experiments to have significantly increased macromolecular mobility compared to a control homogeneous PEO gel. This process allows a means to increase macromolecular transport rates without reducing the crosslink density in the PEO domains.

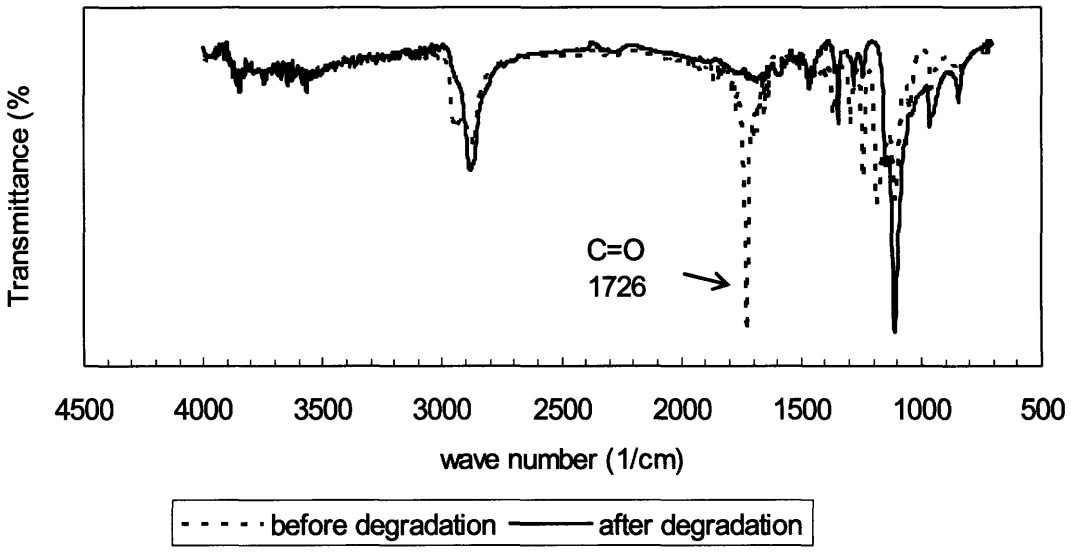

Figure 4.5. FTIR of E45CL30 before (*dotted line*) and after (*solid line*) PCL degradation.

Table 4.2. Penetrant molecules used.

	$D_\infty (10^{-7}\ cm^2/s)^a$	$r_s (nm)^b$
Dye (Acid yellow 73)	43.08 ± 1.83	0.57
Parvalbumin (12 *kDa*)	17.74	1.38
BSA (68 *kDa*)	6.45 ± 0.14	3.80
Carboxylated polystyrene bead	1.80 ± 0.11	13.60

[a] determined by FRAP experiments; [b] calculated from D_∞.

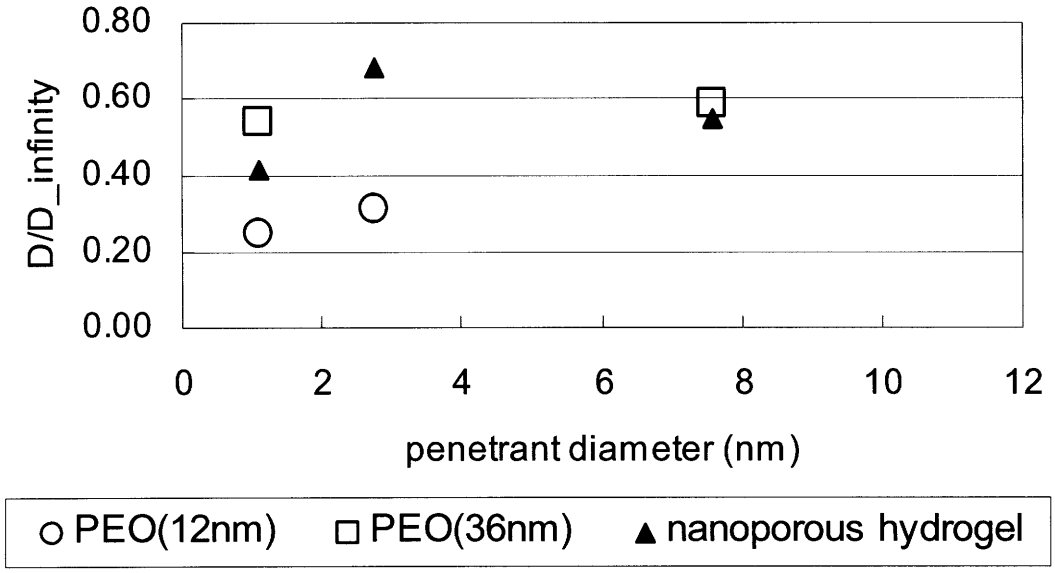

Figure 4.6. Reduced diffusivities for various penetrants; D_∞ is diffusion coefficient in water; PEO (12 *nm*) denotes the PEO network whose mesh size is ~12 *nm*, and the nanoporous hydrogel was synthesized under the similar conditions as for PEO (12 *nm*); no significant penetration of ~8 *nm* probe in 12 *nm* PEO hydrogel has observed.

5. Effect of Temperature and Water on Microphase Separation of PCL-PEO-PCL Triblock Copolymers

1. Introduction

Amphiphilic block copolymers, especially those containing polyethylene oxide (PEO) as a hydrophilic component, have been studied extensively due to their biomedical applications. For example, PEO/poly(ε-caprolactone) (PEO/PCL) block copolymers have been used in drug delivery systems due to the biocompatibility of PEO and PCL and the biodegradability of PCL. Drug loading and release behavior have been reported (Yoo, 1999; Ge, 2002; Yu, 2005) in addition to the kinetics of enzymatic degradation (Gan, 1999; Zhao, 1999; Nie, 2003). PEO and PCL are semi-crystalline, and the thermal properties of the PEO/PCL block copolymers in bulk have been studied (Gan, 1996; Gan, 1997; Bogdanov, 1998; An, 2001; Piao, 2003). Micellar self-assembly of PEO/PCL block copolymers in dilute aqueous solutions has been also reported (Zhao, 2001). The phase behavior of low molecular weight PEO/PCL block copolymers was studied at low polymer concentrations up to 35% (Hwang, 2005; Bae, 2005), however, most studies of phase behavior have been limited to either dilute solutions or to bulk systems, yet recently concentrated solutions have been used to form nanostructured and porous hydrogels (Kang, 2006).

In our study, various concentrations (20-80 wt %) and high molecular weights of PCL-*b*-PEO-*b*-PCL were used to study phase behavior using Small Angle X-ray Scattering (SAXS), Atomic Force Microscopy (AFM), and Differential Scanning Calorimetry (DSC). High concentration studies are useful because the block copolymers exhibit multiple morphologies at high concentrations including lamellae and cylinders (Wanka, 1994). The influence of the crystallinity of both PEO and PCL upon microphase separation was examined both by varying the temperature and by adding water, the latter of which should affect PEO crystallinity more strongly than PCL crystallinity due to its hydrophilic nature.

5. 2. Experimental Section

5.2.1. Materials

PEO, ε-caprolactone, and stannous octoate were purchased from Sigma-Aldrich and used without further purification. Sodium azide and methanol were purchased from Mallinckrodt (Phillipsburg, NJ), and the solvents (dichloromethane, *n*-hexane) were obtained from EMD Chemicals (Gibbstown, NJ).

5.2.2. Synthesis of PCL-*b*-PEO-*b*-PCL triblock copolymers

10 g of PEO was reacted with 17 ml of ε-caprolactone in the presence of stannous octoate (3 drops) as a catalyst at 130°C for 21 hours under a nitrogen atmosphere. A synthesized block copolymer was purified with dichloromethane and cold *n*-hexane three times. The final product was dried in a hood at room temperature for one day and in a vacuum oven at 40°C for another two days. The polymerization yield was 33%. Table 5.1 shows a poly(ε-caprolactone-*b*-ethylene oxide-*b*-ε-caprolactone) (PCL-PEO-PCL) block copolymer, whose molecular weights were determined by ^{1}H-NMR and GPC. The block copolymer is denoted as E30CL36, signifying that 30,000 g/mol of PEO was used, and that the volume percent of PCL is 36%.

5.2.3. Morphology of PCL-b-PEO-b-PCL triblock copolymers

The morphologies of the dried powder samples of the block copolymer were studied after drying the purified polymer solutions (mainly in dichloromethane as a solvent) in a hood at room temperature for one day and in a vacuum oven at 40°C for another two days. The synthesis and purification of the polymer in addition to solvent evaporation were repeated twice, and those separately-prepared powder samples yielded reproducible morphology results obtained using Small Angle X-ray Scattering (SAXS) (described in more detail in the Characterization section). Aqueous polymer samples were prepared by adding Milli-Q water with 0.01% NaN_3 to make 20 %, 40 %, 60 %, and 80 % polymer concentrations, and after equilibration at room temperature for a week, morphologies of those samples were studied using SAXS.

Table 5.1. A PCL-*b*-PEO-*b*-PCL triblock copolymer synthesized.

	M_n (PEO)[a] *g/mol*	M_n (NMR)[b] *g/mol*	M_n[c] *g/mol*	M_w/M_n[c]
E30CL36	30,000	9,000-30,000-9,000	43,000	1.17

[a] determined by GPC using starting PEO homopolymer; [b] determined by ^{1}H-NMR based on the M_n of PEO measured by GPC; [c] from GPC.

5.2.4. Crosslinking of PCL-b-PEO-b-PCL by electron beam irradiation

Milli-Q water with 0.01% NaN_3 was added to PCL-*b*-PEO-*b*-PCL in a 5 *cm* diameter Petri dish to form a solution of 80% polymer concentration. After equilibration at room temperature for a week, the aqueous solution underwent electron beam irradiation to crosslink primarily the PEO block in the block copolymer (Kang, 2006). A 50 *Mrad* dose was applied, and the temperature during irradiation was not controlled. A crosslinked sample was extracted with 0.01% NaN_3 Milli-Q water, and dried in a vacuum oven at 40°C for two days.

5.2.5. Characterization

Number and weight average molecular weights (M_n and M_w, respectively) and polydispersities (M_w/M_n) were obtained using a Waters Gel Permeation Chromatograph (GPC) at the University of Akron using tetrohydrofuran (THF) as the solvent at a 1 *ml/min* elution rate with calibration through use of polystyrene standards. Small Angle X-ray Scattering (SAXS) experiments were performed at the Institute for Soldier Nanotechnologies (ISN) at MIT. Wet samples of triblock copolymers (emulsions in water) were enclosed in Kapton™ tape. SAXS data were collected for exposures of 1,000 *sec*. Background calibration was performed by subtracting the signals from the corresponding empty Kapton™ tape holders. Scattering data were analyzed using Datasqueeze™ and integrated using the "average" function. The "sum" integration method was used for Figure 5.1 and Figure 5.7 to make the peaks more pronounced in the graphs; however, the peak positions were same as the integration results obtained using "average." An Atomic Force Microscopy (AFM) image was taken with a Veeco Metrology Group Nanoscope IV Scanning Probe Microscope (Digital Instruments) at the MIT Center for Material Science and Engineering (CMSE). A dry sample was microtomed to produce a smooth surface for AFM measurement. Melting peaks (T_m) and crystallization peaks (T_c) of the block copolymer were obtained with a Perkin Elmer Pyris 1 Differential Scanning Calorimeter (DSC) at CMSE. Powder samples of 5-10 mg were enclosed in aluminum pans and were heated at the rate of 10°C/*min* from

20°C to 100°C, held at 100°C for 3 min, and cooled at the rate of 10°C/*min* to 20°C. These samples were heated again to 100°C at the same rate to collect the DSC results for the heating cycle, so as to erase previous thermal history. Aqueous samples are prepared using high pressure stainless steel pans with O-rings to prevent the evaporation of water.

5.3. Results and Discussion

5.3.1. Microphase separation of the block copolymer by solvent evaporation

Microphase separation of the block copolymer, E30CL36 (Table 5.1), was induced by solvent (dichloromethane) evaporation at room temperature for one day and by further drying at 40°C for two days. Crystallization of PEO of the block copolymer competes with the microphase separation process (An, 2001) because the morphology induced by microphase separation raises free energy of crystalline phase, most likely through domain size associated surface free energy. E30CL36 has a 36% volume fraction of PCL, and its microphase separation was studied using SAXS (Figure 5.1). It shows three peaks whose q ratios are $1:\sqrt{3}:\sqrt{7}$. The expected q ratio for a cylindrical microphase is $1:\sqrt{3}:\sqrt{4}:\sqrt{7}\ldots$ (Chu, 2001), but as peaks positions for $\sqrt{3}$ and $\sqrt{4}$ lie close together, the sample is identified as having a cylindrical morphology (cylinders of PCL in PEO matrix) despite of the absence of a separate identifiable peak at the $\sqrt{4}$ position.

5.3.2. Effect of temperature on morphology of E30CL36

The melting behavior of *E30CL36* powder samples was studied using DSC. PCL homopolymer, 8,000 g/mol, has a melting peak (T_m) at 59°C (Piao, 2003), while PEO homopolymer, 30,000 g/mol has a T_m at 67°C (Figure 5.2). However, the block copolymer, E30CL36, exhibited lower T_m's as shown in Figure 5.3. The T_m of PEO was reduced to 61 °C probably due to the imperfect crystallization rendered by microphase separation, while the T_m of PCL was observed at ~54°C. PCL crystallinity was suppressed significantly due to the shorter block length of PCL than that of PEO (Figure 5.3). Comparable results were reported by Gan (1996), who suggested that the shorter PEO block length than that of PCL (20 weight

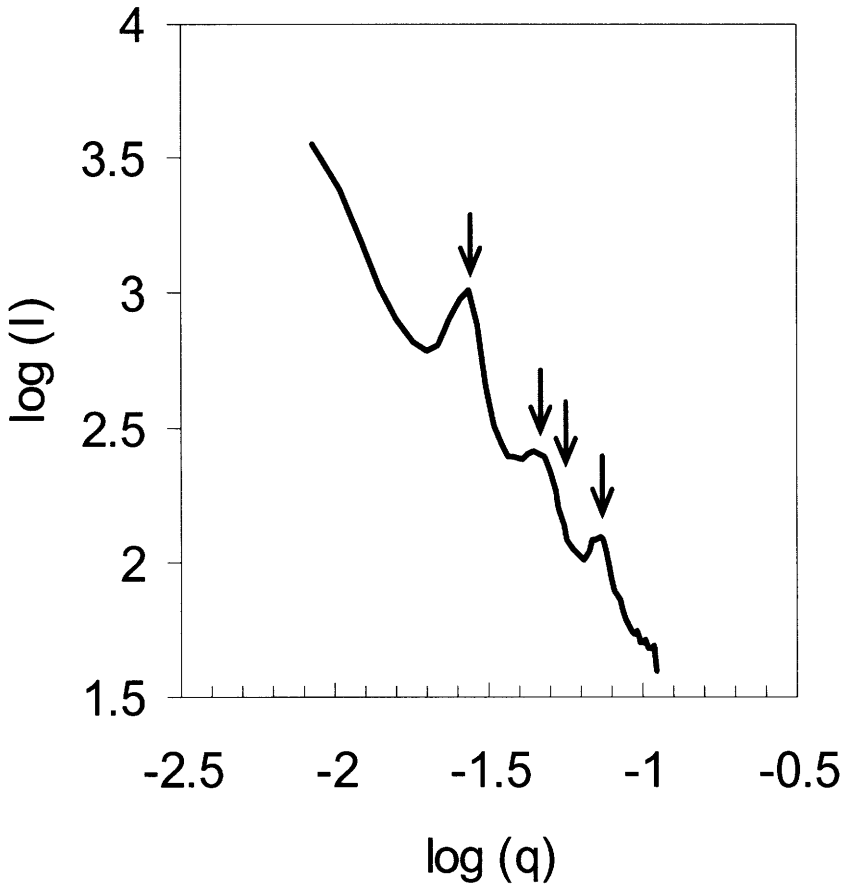

Figure 5.1. SAXS of *E30CL36* powders prepared by solvent evaporation; the arrows are expected peak positions for a cylindrical microphase; the first order peak is 24 nm.

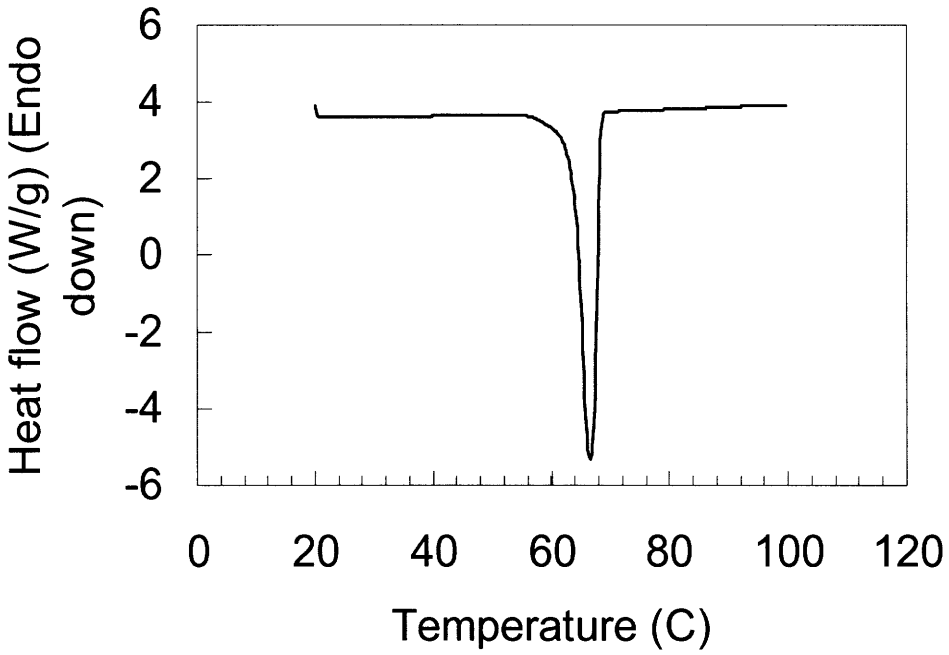

Figure 5.2. DSC of PEO homopolymer powders (30 000g/mol); the second heat cycle of DSC is shown; the melting peak is observed at 67°C.

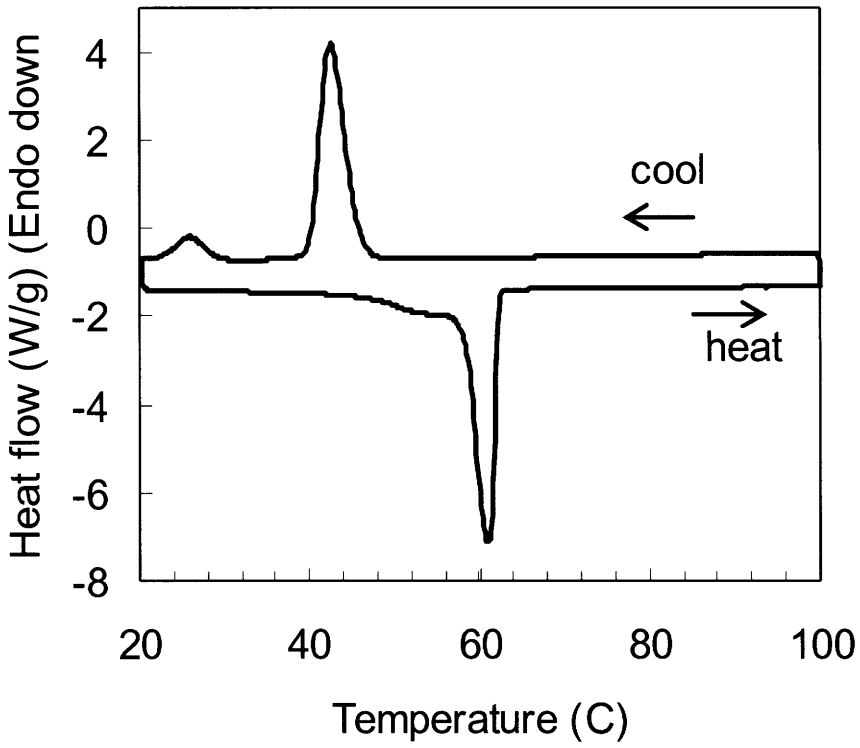

Figure 5.3. DSC of *E30CL36* powders; the second heat cycle of DSC is shown in addition to the cooling cycle; the first melting peak is the T_m of PCL (54°C), while the second at 61°C is the T_m of PEO; in the cooling cycle, $T_{c,PCL}$=25°C and $T_{c,PEO}$=42°C.

% PEO) in their PEO-*b*-PCL sample resulted in complete suppression of PEO crystallinity. The cooling cycle also shows two crystallization peaks, and the peak at 42°C is that of PEO. Presence of both crystallization peaks of PEO and PCL in addition to melting peaks of PEO and PCL further confirms microphase separation of the block copolymer. The effect of temperature on microphase separation of the block copolymer was studied using SAXS (Figure 5.4). Powder samples of E30CL37 were enclosed in Kapton Tape™, and mounted on a hot stage to increase the temperature to 70°C. Before collecting scattering data, samples were equilibrated at each reported temperature for 30 min. At low temperatures, three peaks were observed, and their q ratios are $1:\sqrt{3}:\sqrt{7}$, indicating a cylindrical morphology. This morphology is retained until melting of PEO and PCL occurs. After melting at ~60°C, the first order peak decreased to a lower q, representing an increase in the domain size, but the changed morphology could not be identified due to the presence of only one peak. The block copolymer is expected to have an equilibrium morphology at temperatures above the melting points of both blocks. The mean-field theory suggests that the block copolymer has a gyroid microphase as the volume fraction of PCL is 36% (Bates, 1999). Therefore, the change in morphology observed at temperatures above melting points of PEO and PCL suggests that the cylindrical morphology obtained by solvent evaporation at below the melting points was determined kinetically through competition between microphase separation and the crystallization of PEO and PCL. The kinetically captured cylindrical morphology was reproducible upon multiple observations.

An as-cast sample of the block copolymer was heated at 70°C for one day to melt the crystalline structures, and then re-cooled to room temperature at ambient atmosphere. The resulting sample was investigated by SAXS, and it was found that the sample has a lamellar morphology as shown in Figure 5.5. This is perhaps because PCL blocks crystallize faster than PEO blocks because PEO is blocked by PCL at both ends. And this produces PCL crystalline lamellae next to PEO amorphous regions (Gan, 1996; Nojima, 1997; Perret, 1972). Slow cooling is expected to produce more complete microphase separation, and PEO will crystallize within microphase-separated structures (An, 2001). When water is added to decrease the polymer concentration to 80%, the lamellar morphology is retained, and the length scale of the lamellae increases to 29 nm from 27 nm due to swelling of the PEO.

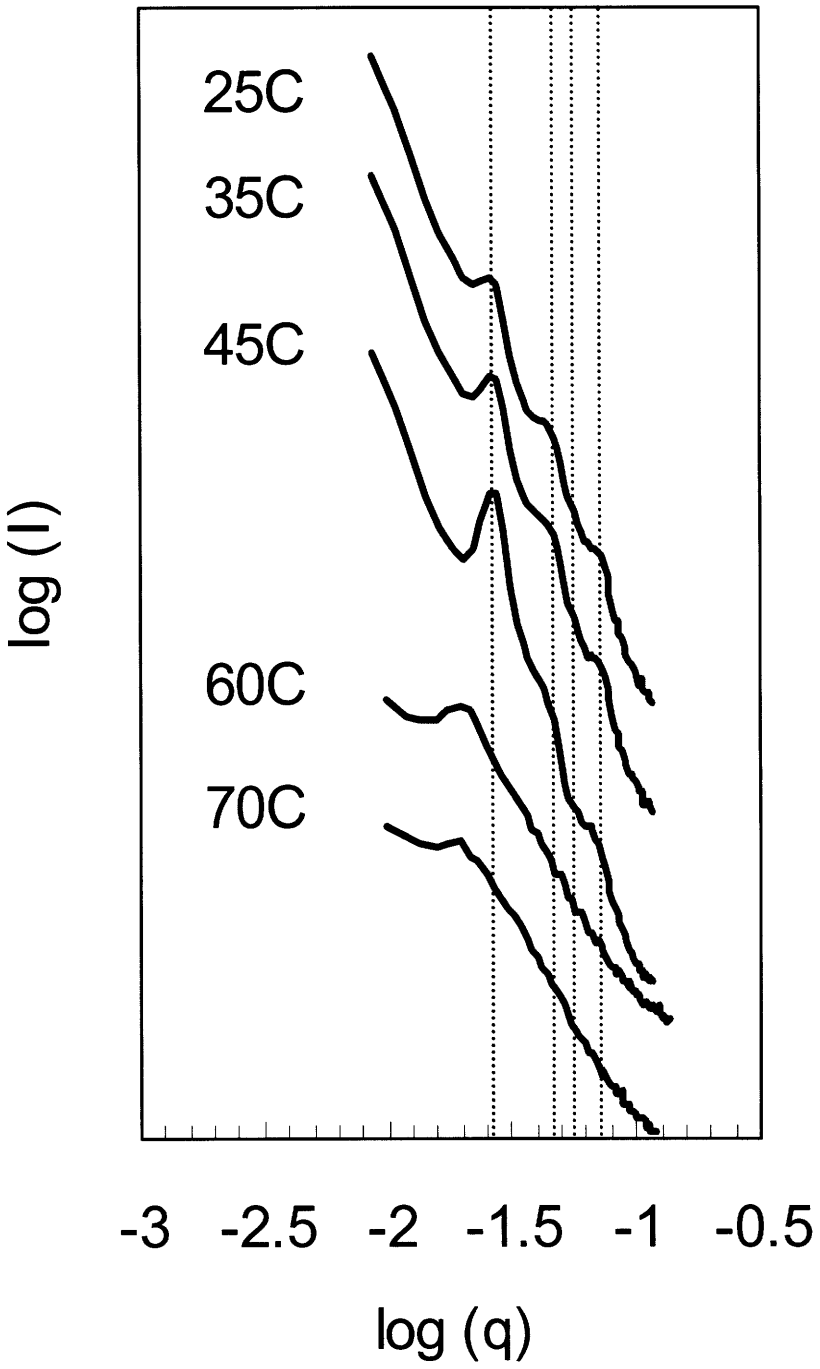

Figure 5.4. SAXS of *E30CL36* powders; the dotted lines are expected peak positions for a cylindrical microphase; the first order peaks are 24nm for 25°C, 35°C, and 45°C, and 31nm for 60°C and 70°C.

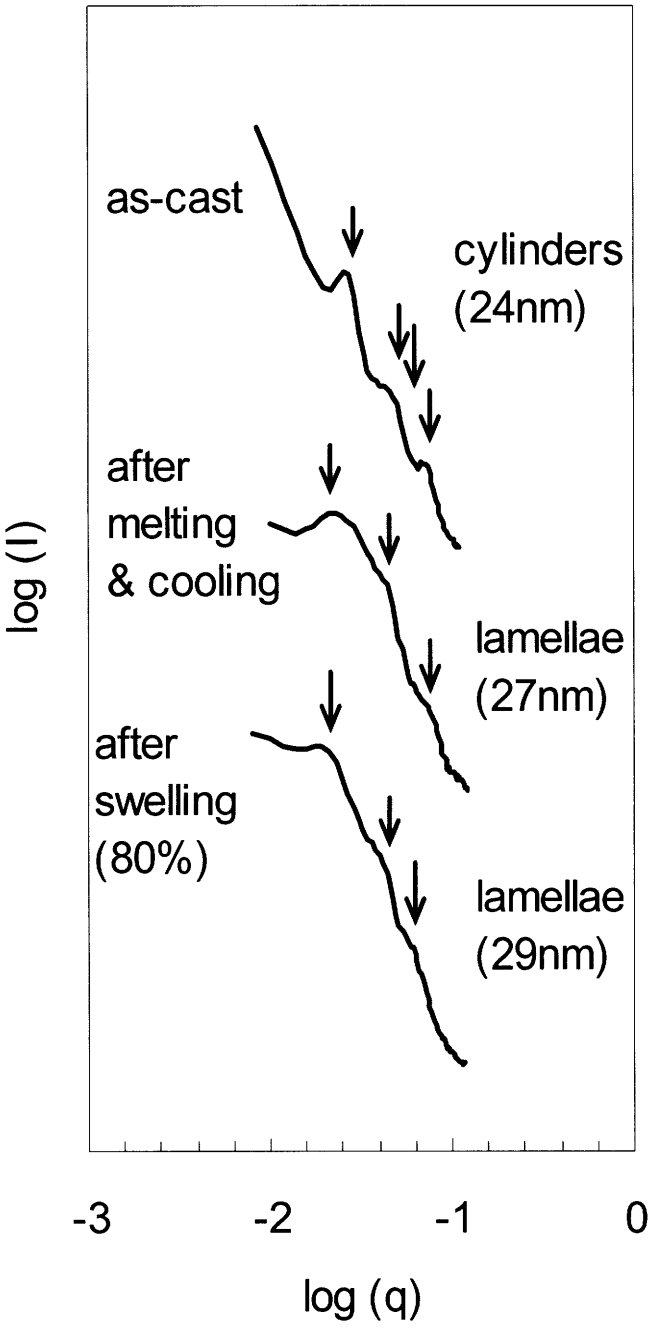

Figure 5.5. SAXS of *E30CL36* at room temperature; the arrows are expected peak positions for an indicated morphology; 80% indicates 80% polymer concentration in water.

The lamellar structures of E30CL36 were also observed by AFM. The sample for AFM was prepared by crosslinking the block copolymer at 80% polymer concentration by electron beam irradiation to fix the microstructure. Figure 5.6 shows an AFM phase image of the sample in a dry state. The domain size of the lamellar structure is 23nm.

5.3.3. Effect of water on morphology of E30CL36

Good solvent reduces the melting points of crystalline polymers, and is mixed with the polymer chains in the amorphous regions (Sharples, 1966). The effect of water on the hydrophilic PEO homopolymer (M_n=15,000 g/mol) was studied using DSC. In the bulk phase, it has a T_m peak at 66°C. However, when water is added to decrease the polymer concentration to 80%, the T_m decreases to 51°C (Figure 3.9). Futhermore, as more water was added to reduce the polymer concentration further to 20%, the melting peak disappeared, suggesting complete suppression of PEO crystallinity. Since PCL-*b*-PEO-*b*-PCL is amphiphilic, water can produce interesting morphology changes in the block copolymer systems. Previously, it was described that the shorter PCL block than that of PEO resulted in significant suppression of PCL crystallinity. When water is added to the block copolymer, water will increase the amorphous regions of PEO, and hence improve PEO mobility. This may improve PCL crystallization and PCL crystalline lamellae formation may be enhanced considerably.

To study the effect of water on the crystallinity of PCL-PEO-PCL block copolymer, DSC experiments were performed at various polymer concentrations (Figure 5.7). As described previously, the bulk (100% concentration) sample has crystallization peaks of both PCL and PEO (25°C and 42°C, respectively). At 80% polymer concentration, the T_c of PEO decreased, and the T_c of PCL increased which made it overlapping with that of PEO. The crystallization peak height of PEO also decreased relative to that of PCL, suggesting the crystallization portion was reduced and the amorphous region increased. When more water was added to make 60% polymer concentration, two crystallization peaks were completely overlapped.

The effect of water upon the block copolymer morphology was studied using SAXS (Figure 5.8). As described above, a bulk (100% concentration) sample of the block

copolymer exhibits a cylindrical morphology following solvent evaporation. When water was added to reduce the concentration to 80% followed by a week of equilibration, the cylindrical morphology was retained with a slight increase in length scale due to swelling of PEO by water. However, as more water was added to reduce the polymer concentration to 60%, a dramatic morphology change occurred. The 60% SAXS spectrum shows three peaks, and the q ratios are 1:2:3, indicating lamellar structures. This morphology remains with 20% and 40% samples. The morphology change from cylinders to lamellae is probably related to decreased PEO crystalline portion, hence increased amorphous region.

These SAXS and DSC data suggest that water reduces PEO crystallinity and increases PEO mobility, hence might improve PCL crystallinity that was suppressed by PEO crystallization. This suggested idea was schematically drawn in Figure 5.9. In the figure, water increases an amorphous portion of PEO and mixes with the PEO chain in the amorphous regions only (Sharples, 1966). This amorphous region improves PEO mobility, and makes it easier to form PCL crystalline lamellae, resulting in lamellar microphase separation between PEO and PCL in the block copolymer. Unfortunately, few studies have been reported about morphologies of PEO/PCL block copolymers when both blocks are comparably crystalline. An (2001) used SAXS to study a morphology change between two different crystallization temperatures, however, they did not succeed in identifying the morphology observed at the ~18 nm length scale due to experimental difficulties. Further studies are required to understand better the morphology effect of water addition.

5.4. Conclusions

The microphase separation of PCL-*b*-PEO-*b*-PCL (M_n= 9,000-30,000-9,000 g/mol, f_{PCL}=0.36) was studied using SAXS, AFM, and DSC. The morphologies of the block copolymer at room temperature were determined by competition between microphase separation and crystallization of PEO and PCL. Two different morphologies (cylinders and lamellae) were observed at room temperature in addition to the unidentified one at temperatures above melting points of both blocks. A cylindrical morphology was formed by solvent evaporation of the block copolymer at room temperature and annealing at 40°C. Lamellae were observed after the block copolymer was melted and cooled to room

temperature. Addition of water at room temperature also changed the morphology from cylinders to lamellae.

Figure 5.6. AFM phase image of crosslinked *E30CL36* at 80% polymer concentration; image size is 1μm x 1μm, and a domain size of the lamellae is 23nm (dry sample).

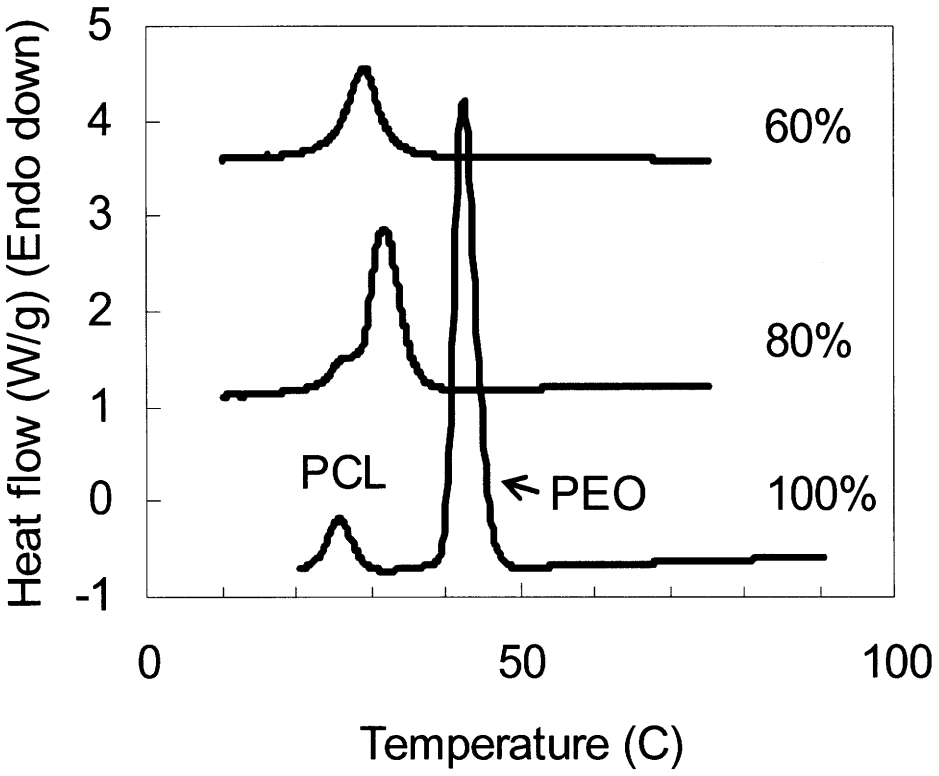

Figure 5.7. DSC cooling curves of *E30CL36*; in a 100% sample, the crystallization peak at 25°C is Tc of PCL, while the one at 42°C is that of PEO; for 60% and 80% aqueous samples, 5°C/min cooling rate was used, while 10°C/min was used for a 100% sample.

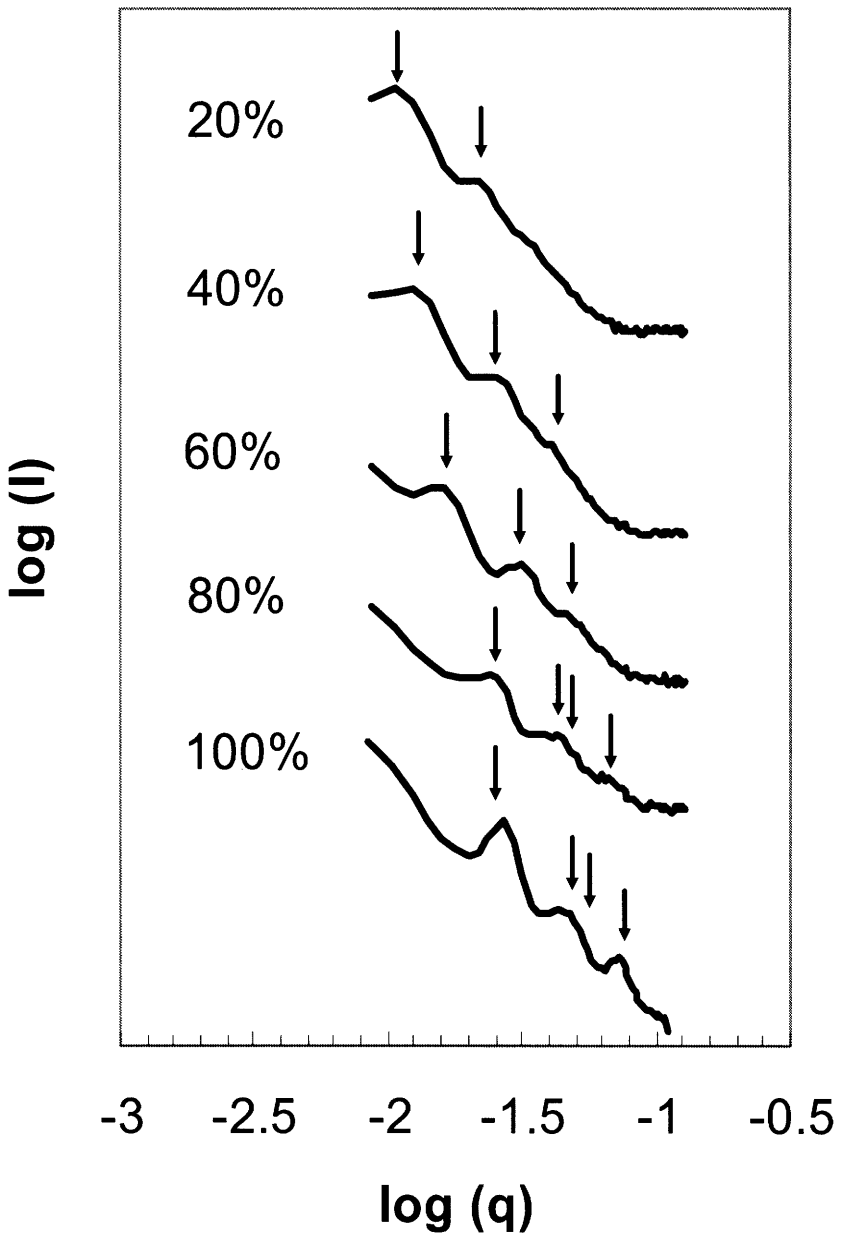

Figure 5.8. SAXS of *E30CL36* in water at various polymer concentrations; the arrows for 20%, 40%, and 60% are expected peak positions for a lamellar microphase, while 80% and 100% a cylindrical microphase; the first order peak for 20%, 40%, 60%, 80%, and 100% are 52 *nm*, 45 *nm*, 40 *nm*, 25 *nm*, and 24*nm* respectively.

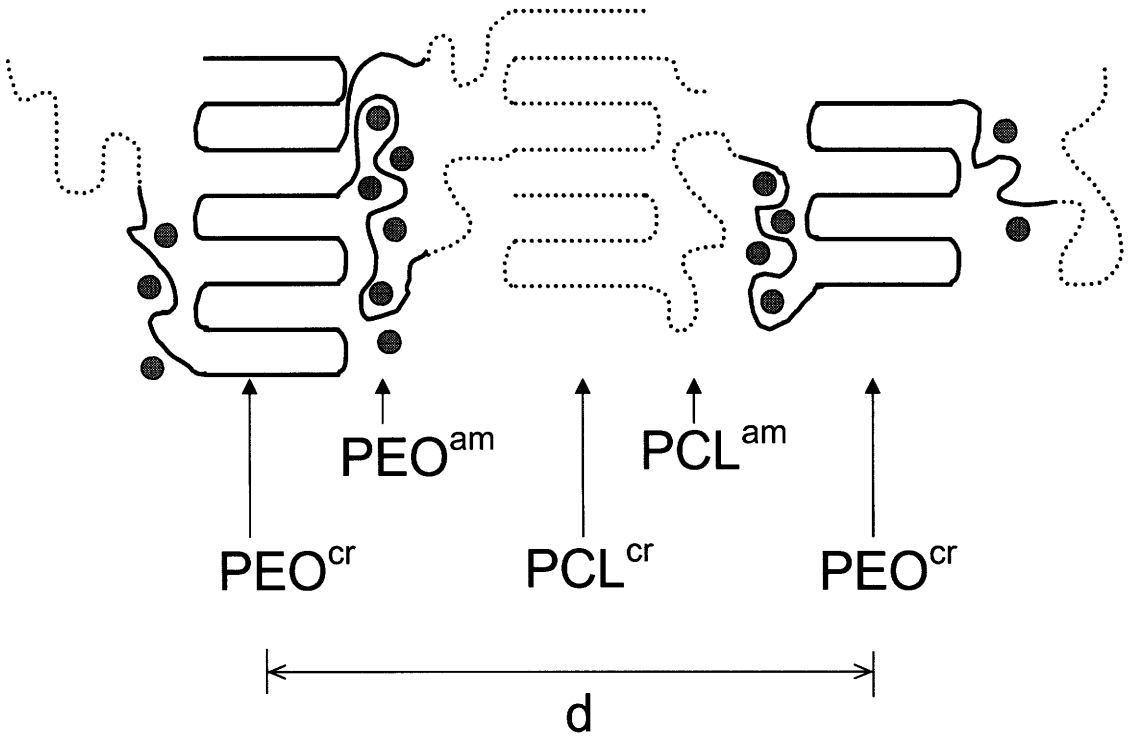

Figure 5.9. Brief schematic drawing of the lamellar morphology of *E30CL36* at 60% polymer concentration; gray dots denote water molecules.

6. Conclusions and Recommendations

6.1. Synthesis and Characterization of PCL-b-PEO-b-PCL Based Nanostructured and Porous Hydrogels

- Conclusions: Nanostructured and porous PEO hydrogels were synthesized using amphiphilic PCL-*b*-PEO-*b*-PCL triblock copolymers. After microphase separation of the triblock copolymers in water, crosslinking of the PEO block was performed with an electron beam, followed by PCL removal through hydrolysis. Microphase structures were observed by SAXS (emulsion samples) and AFM (cross-linked samples); these were mostly lamella yet cylindrical in one instance. SAXS experiments following PCL removal showed no significant structure, perhaps due to a lack of contrast in swollen states of the "porous" hydrogels. These nanostructured and porous hydrogels have hydroxyl functional groups available for further chemical modification and can be used in biomedical or pharmaceutical applications.

- Future work: Modification of hydroxyl groups of the nanostructured and porous hydrogels with pH or temperature responsive materials would be an interesting future work. They may be used in biomedical areas such as drug delivery after reacting to temperature or pH responsive materials to further control pores size depending on the environment where the hydrogels are used. The hydrophilicity and biocompatibility of these hydrogels are advantageous for this application. These hydrogels can also be used as matrix to immobilize enzymes, which are essential for biological reactions. When they are immobilized, their recovery from reactants and products is easy and they can be reused.

  Hydroxyl groups of the nanostructured and porous hydrogels can directly react with carboxyl groups of the materials that are to be attached. For example, they can react with a carboxyl group of an amino acid, and by reacting an amine group of the amino acid with a carboxyl group of another amino acids, a polypeptide chain will form (Scheme 6.1 (a), Montalbetti, 2005). The hydrogel makes it easy to wash off

undesired reactants and byproducts from the reaction solution so that a desired polypeptide sequence can be produced. Furthermore, they can be modified to produce other reactive materials so they can be reacted with amine groups of materials that are to be attached. For example, S-triazine derivatives or p-benzoquinone can react to –OH group of the hydrogel to produce reactive intermediates (Scheme 6.1 (b) and (c)). This intermediate further reacts to amine terminal groups of proteins.

In addition, pH responsive hydrogels have been used for insulin delivery. For example, glucose-sensitive hydrogels swell/deswell depending on glucose concentration in the blood to release insulin. This swell/deswell behavior is controlled by pH because when glucose reacts with an enzyme (glucose oxidase), gluconic acid is produced, and pH of the medium decreases. For a pH responsive material, the hydrogels contain cationic polyelectrolytes or anionic polyelectrolytes. Polycationic polymers swell when pH decreases, and polyanionic hydrogels collapse when pH decreases. Glucose oxidase is entrapped or immobilized on the hydrogels for a rapid pH change depending on glucose concentration. For insulin delivery, both polycationic hydrogels (Klumb, 1992) and polyanionic hydrogels (Cartier, 1995) were used. Polycationic hydrogels capped a flexible insulin reservoir so that insulin can be released when the hydrogels swell as pH decreases. Polyanionic hydrogels were immobilized to a cylindrical monolith that contains insulin. When pH decreases, the hydrogels collapses and the pores open. Glucose-sensitive hydrogels can also be used without a reservoir when the hydrogels contain insulin (Podual, 2000a, 2000b; Goldbart, 2002).

Using our nanostructured and porous hydrogels can improve this insulin delivery further by utilizing heterogeneous pores (produced by PCL removal). Modifying hydroxyl groups of the hydrogel with pH-responsive materials will result in pore opening/closing depending on pH change. Furthermore, due to the pores, the swelling/deswelling behavior will be faster than conventional hydrogels. Relatively slow swelling/deswelling of conventional polycationic hydrogels was observed in the study by Podual (2000, b). Bulk diffusion of water through pores is expected to

resolve this issue (Albin, 1985). Therefore, the nanostructured and porous hydrogels will improve this issue.

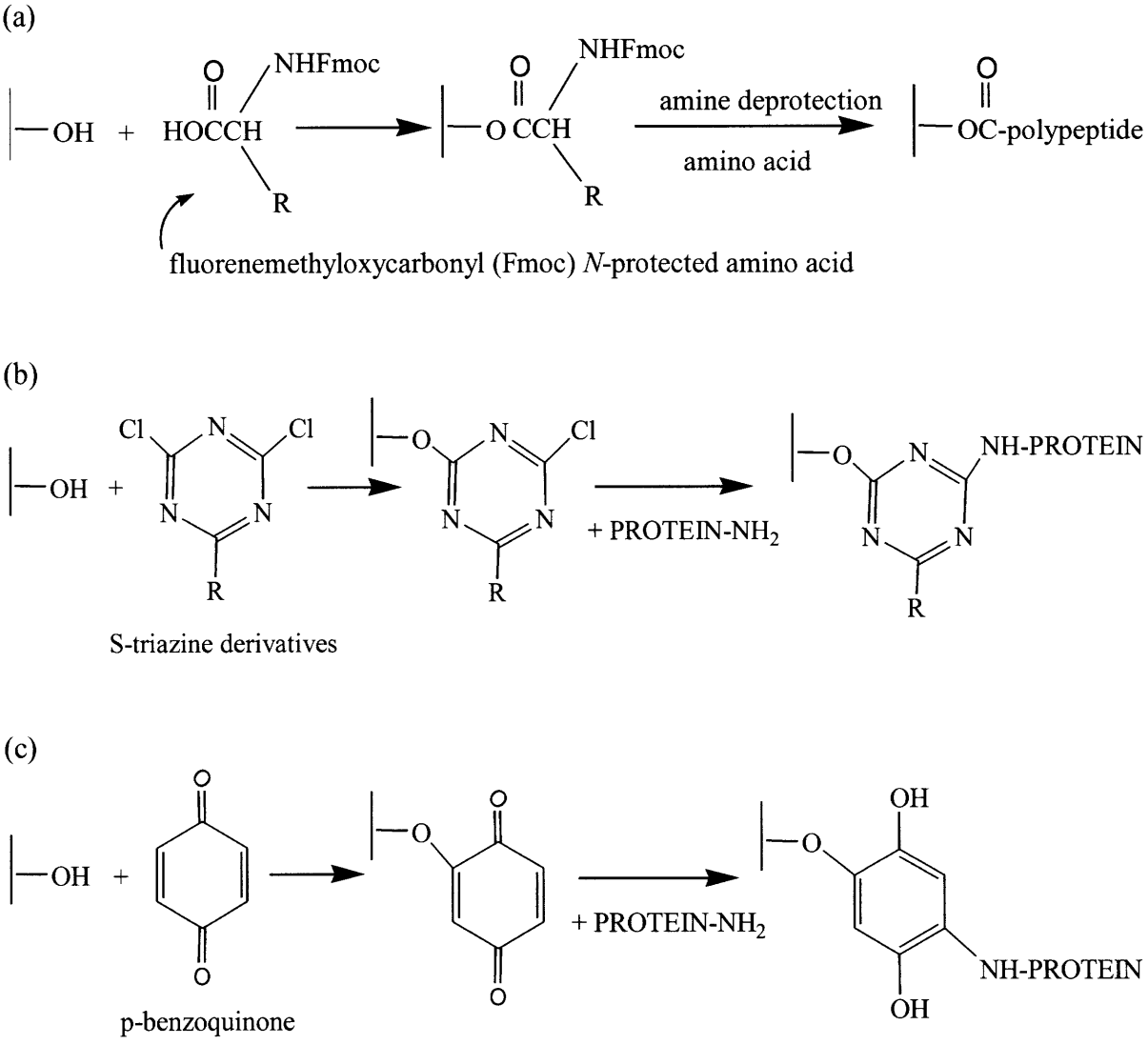

Scheme 6.1. Modification of hydroxyl functional groups of the nanostructured and porous hydrogels; (a) a carboxyl group of amino acid reacts with –OH of the hydrogel; a protected amine group of the amino acid with fluorenemethyloxycarbonyl group reacts with other amino acid after deprotection to produce a polypeptide chain (Montalbetti, 2005); (b) S-triazine derivatives react with –OH of the hydrogel to produce reactive intermediate that can react with an amine group of proteins or enzymes (Shulder, 1992); (c) p-benzoquinone reacts with –OH of the hydrogel to produce reactive intermediate that can react with an amine group of proteins or enzymes (Brandt, 1975).

6.2. Macromolecular Transport through Nanostructured and Porous Hydrogels Synthesized Using the Amphiphilic Copolymer, PCL-b-PEO-b-PCL

- Conclusions: A nanostructured and porous hydrogel was synthesized using high molecular weights of PCL-*b*-PEO-*b*-PCL block copolymer. An emulsion of the block copolymer in water was crosslinked in an electron beam and exhibited lamellar morphology. The PCL domains were then removed through hydrolysis. The regions formerly occupied by PCL offer additional channels for macromolecular transport through the gel. A hydrogel with this nanostructured porosity was found through FRAP experiments to have significantly increased macromolecular mobility compared to a control homogeneous PEO gel. This process allows a means to increase macromolecular transport rates without reducing the crosslink density in the PEO domains.

- Future work: Mechanical measurement studies of these hydrogels would be interesting. Swelling ratio data, which have relatively close relationship with mechanical strength of hydrogels, suggest that the nanoporous hyrogels might have stronger mechanical strength than the homogeneous PEO hydrogel that has similar transport properties.

6.3. Effect of Temperature and Water on Microphase Separation of PCL-PEO-PCL Triblock Copolymers

- Conclusions: The microphase separation of PCL-*b*-PEO-*b*-PCL (M_n= 9,000-30,000-9,000 g/mol, f_{PCL}=0.36) was studied using SAXS, AFM, and DSC. The morphologies of the block copolymer at room temperature were determined by competition between microphase separation and crystallization of PEO and PCL. Two different morphologies (cylinders and lamellae) were observed at room temperature in addition to the unidentified one at temperatures above melting points of both blocks. A cylindrical morphology was formed by solvent evaporation of the block copolymer at room temperature and annealing at 40°C. Lamellae were observed after the block

copolymer was melted and cooled to room temperature. Addition of water at room temperature also changed the morphology from cylinders to lamellae.

- Future work: Investigating morphology change of the block copolymers at temperatures above melting points of each block would be interesting to see which block of the block copolymer is the dominant one for morphology change. And the identification of the morphology observed at temperatures above melting points of both PEO and PCL by AFM or SEM will be useful.

Biobliography

Albin, G.; Horbett, T. A.; Ratner, B. D., "Glucose sensitive membranes for controlled delivery of insulin: Insulin transport studies," *J. Control. Release.* **1985**, *2*, 153.

An, J. H.; Kim, H. S.; Chung, D. J.; Lee, D. S.; Kim, S., "Thermal behaviour of poly(ε-caprolactone)-poly(ethylene glycol)-poly(ε-caprolactone) tri-block copolymers," *J. Mater. Sci.* **2001**, *36*, 715.

Bae, S. J.; Suh, J. M.; Sohn, Y. S.; Bae, Y. H.; Kim, S. W.; Jeong, B., "Thermogelling poly(caprolactone-*b*-ethylene glycol-*b*-caprolactone) aqueous solutions," *Macromolecules.* **2005**, *38*, 5260.

Barakat, I.; Dubois, P. H.; Grandfils, C. H.; Jerome, R., "Macromolecular engineering of polylactones and polylactides. XXV. Synthesis and characterization of bioerodible amphiphilic networks and their use as controlled drug delivery systems," *J. Polym Sci.: Polym. Chem.* **1999**, *37*, 2401.

Bates, F. S.; Fredrickson, G. H., "Block copolymers-designer soft materials," *Physics today* **1999**, *52*, 32.

Bogdanov, B.; Vidts, A.; Van Den Bulcke, A.; Verbeeck, R.; Schacht, E., "Synthesis and thermal properties of poly(ethylene glycol)-poly(ε-caprolactone) copolymers," *Polymer* **1998**, *39*, 1631.

Bovey, F. A. The effects of inonizing radiation on natural and synthetic high polymers, polymer review series vol I; Interscience: New York, 1958; p. 174.

Brandt, J.; Andersson, L.-O.; Porath, J., "Covalent attachment of proteins to polysaccharide carriers by means of benzoquinone," *Biochem. Biophys. Acta* **1975**, *386*, 196.

Campos, A.; Franchetti, S. M. M., "Biotreatment effects in films and blends of PVC/PCL previously treated with heat," *Braz. Arch. Biol. Technol.* **2005**, *48*, 235.

Canal, T.; Peppas, N. A., "Correlation between mesh size and equilibrium degree of swelling of polymeric networks," *J. Biomed. Mater. Res.* **1989**, *23*, 1183.

Cartier, S.; Horbett, T. A.; Ratner, B. D., "Glucose-sensitive membrane coated porous filters for control of hydraulic permeability and insulin delivery from a pressurized reservoir," *J. Membr. Sci.* **1995**, *106*, 17.

Cavicchi, K. A.; Zalusky, A. S.; Hillmyer, M. A.; Lodge, T. P., "An ordered nanoporous monolith from an elastomeric crosslinked block copolymer precursor," *Macromol. Rapid. Commun.* **2004**, *25*, 704.

Cheng, Y.; Prud'homme, R. K.; Thomas, J. L., "Diffusion of mesoscopic probes in aqueous polymer solutions measured by fluorescence recovery after photobleaching," *Macromolecules* **2002**, *35*, 8111.

Chu, B.; Hsiao, B. S., "Small-angle X-ray scattering of polymers," *Chem. Rev.* **2001**, *101*, 1727.

Cohn, D.; Stern, T.; Gonzalez, M. F.; Epstein, J., "Biodegradable poly(ethylene oxide)/poly(ε-caprolactone) multiblock copolymers," *J. Biomed. Mater. Res. A.* **2002**, *59*, 273.

Collins, E. A.; Bareš, J.; Billmeyer, Jr. F.W. Experiments in polymer science; Wiley: New York, 1973.

De Clercq, R. R.; Goethals, E. J., "Polymer networks containing degradable polyacetal segments," *Macromolecules* **1992**, *25*, 1109.

De Smedt, S. C.; Meyvis, T. K. L.; Demeester, J.; Van Oostveldt, P.; Blonk, J. C. G.; Hennink, W. E., "Diffusion of macromolecules in dextran methacrylate solutions and gels as studied by confocal scanning laser microscopy," *Macromolecules* **1997**, *30*, 4863.

Dennison, K. A. Radiation Crosslinked Poly(ethylene oxide) Hydrogel Membranes. Ph.D. Thesis, Massachusetts Institue of Technology, 1986;chapter 3.

Doytcheva, M.; Dotcheva, D.; Stamenova, R.; Orahovats, A.; Tsvetanov, C.; Leder, J., "Ultraviolet-induced crosslinking of solid poly(ethylene oxide)," *J. Appl. Polym. Sci.* **1997**, *64*, 2299.

Erdodi, G.; Kennedy, J. P., "Ideal tetrafunctional amphiphilic PEG/PDMS conetworks by a dual-purpose extender/crosslinker. II. Characterization and properties of water-swollen membranes," *J. Polym Sci.: Polym. Chem.* **2005**, *43*, 4965.

Gan, Z.; Jim, T. F.; Li, M.; Yuer, Z.; Wang, S.; Wu, C., "Enzymatic biodegradation of poly(ethylene oxide-*b*-ε-caprolactone) diblock copolymer and its potential biomedical applications," *Macromolecules* **1999**, *32*, 590.

Gan, Z.; Jiang, B.; Zhang, J., "Poly(ε-caprolactone)/poly(ethylene oxide) diblock copolymer. I. Isothermal crystallization and melting behavior," *J. Appl. Polym. Sci.* **1996**, *59*, 961.

Gan, Z.; Zhang, J.; Jiang, B., "Poly(ε-caprolactone)/poly(ethylene oxide) diblock copolymer. II. Nonisothermal crystallization and melting behavior," *J. Appl. Polym. Sci.* **1997**, *63*, 1793.

Ge, H.; Hu, Y.; Jiang, X.; Cheng, D.; Yuan, Y.; Bi, H.; Yang, C., "Preparation, characterization, and drug release behaviors of drug nimodipine-loaded poly(ε-caprolactone)-poly(ethylene oxide)-poly(ε-caprolactone) amphiphilic triblock copolymer micelles," *J. Pharm. Sci.* **2002**, *91*, 1463.

Goldbart, R.; Traitel, T.; Lapidot, S. A.; Kost, J., "Enzymatically controlled responsive drug delivery systems," *Polym. Adv. Technol.* **2002**, *13*, 1006.

Hedrick, J. L.; Carter, K. R.; Labadie, J. W.; Miller, R. D.; Volksen, W.; Hawker, C. J.; Yoon, D. Y.; Russel, T. P.; McGrath, J. E.; Briber, R. M., "Nanoporous polyimides," *Adv. Polym. Sci.* **1999**, *141*,1.

Hentze, H.-P.; Kramer, E.; Berton, B.; Forster, S.; Antonietti, M.; Dreja, M., "Lyotropic mesophases of poly(ethylene oxide)-*b*-poly(butadiene) diblock copolymers and their cross-linking to generate ordered gels," *Macromolecules* **1999**, *32*, 5803.

Hwang, M. J.; Suh, J. M.; Bae, Y. H.; Kim, S. W.; Jeong, B., "Caprolactonic Poloxamer Analog: PEG-PCL-PEG," *Biomacromolecules* **2005**, *6*, 885.

Ivanova, R.; Lindman, B.; Alexandridis, P., "Effect of glycols on the self-assesmbly of amphiphilic block copolymers in water. 1. Phase diagrams and structure identification," *Langmuir*, **2000**, *16*, 3660.

Ivin, K. J.; Saegusa, T. (Eds.) Ring-opening polymerization, volume 1, Elsevier Applied Science: London, 1984; p.5.

Kang, J.; Beers, K. J., "Synthesis and characterization of PCL-*b*-PEO-*b*-PCL-based nanostructured and porous hydrogels," *Biomacromolecules* **2006**, *7*, 453.

Klumb, L. A.; Horbett, T. A., "Design of insulin delivery devices based on glucose sensitive membranes," *J. Control. Release.* **1992**, *18,* 59.

Knecht, M. R.; Elias, H.-G. *Makromol. Chem.* **1972**, *157*, 1.

Kosto, K. B.; Deen, W. M., "Diffusivities of macromolecules in composite hydrogels," *AIChE J* **2004**, *50*, 2648.

Lee, J.-S.; Hirao, A.; Nakahama, S., "Polymerization of monomers containing functional silyl groups. 7. Porous membranes with controlled microstructures," *Macromolecules*, **1989**, *22*, 2602.

Lustig, S. R.; Peppas, N. A., "Solute diffusion in swollen membranes. IX. Scaling laws for solute diffusion in gels," *J. Appl. Polym. Sci.* **1988**, *36*, 735.

Matsen, M. W.; Schick, M., "Stable and unstable phases of a diblock copolymer melt," *Phys. Rev. Lett.* **1994**, *72*, 2660.

Matsen, M. W.; Thompson, R. B., "Equilibrium behavior of symmetric ABA triblock copolymer melts," *J. Chem. Phys.* **1999**, *111*, 7139.

Montalbetti, C. A. G. N.; Falque, V., "Amide bond formation and peptide coupling," *Tetrahedron* **2005**, *61*, 10827.

Nie, T.; Zhao, Y.; Xie, Z.; Wu, C., "Micellar formation of poly(caprolactone-*block*-ethylene oxide-*block*-caprolactone) and its enzymatic biodegradation in aqueous dispersion," *Macromolecules* **2003**, *36*, 8825.

Nitta, I.; Onishi, S.; Fujimoto, E. Annual Report of Japanese Association for Radiation Research on Polymers; AEC-tr-6231, 1958-59; Vol. 1, p. 320.

Nitta, I.; Onishi, S.; Nakajima, Y. Annual Report of Japanese Association for Radiation Research on Polymers; AEC-tr-6372, 1961; Vol. 3, p. 437.

Nojima, S.; Hashizume, K.; Rohadi, A.; Sasaki, S., "Crystallization of ε-caprolactone blocks within a crosslinked microdomain structure of poly(ε-caprolactone)-*block*-polybutadiene," *Polymer* **1997**, *38*, 2711.

Piao, L.; Dai, Z.; Deng, M.; Chen, X.; Jing, X., "Synthesis and characterization of PCL/PEG/PCL triblock copolymers by using calcium catalyst," *Polymer* **2003**, *44*, 2025.

Park, M.; Harrison, C.; Chaikin, P. M.; Register, R. A.; Adamson, D. H., "Block copolymer lithography: Periodic arrays of ~10^{11} holes in 1 square centimeter," *Science*, **1997**, *276*, 1401.

Park, Y. J.; Lee, J. Y.; Chang, Y. S.; Jeong, J. M.; Chung, J. K.; Lee, M. C.; Park, K. B.; Lee, S. J., "Radioisotope carrying polyethylene oxide-polycaprolactone copolymer micelles for targetable bone imaging," *Biomaterials* **2002,** *23*, 873.

Patrickios, C. S.; Georgiou, T. K., "Covalent amphiphilic polymer networks," *Curr. Opin. Colloid & Interface Sci.* **2003**, *8*, 76.

Perret, R.; Skoulios, A. *Makromol. Chem.* **1972**, *162*, 147.

Podual, K. (a); Doyle III. F. J.; Peppas, N. A., "Preparation and dynamic response of cationic copolymer hydrogels containing glucose oxidase," *Polymer*, **2000**, *41*, 3975.

Podual, K. (b); Doyle III. F. J.; Peppas, N. A., "Glucose-sensitivity of glucose oxidase-containing cationic copolymer hydrogels having poly(ethylene glycol) grafts," *J. Control. Release.,* **2000**, *67*, 9.

Salovey, R.; Dammont, F. R. *J. Polym. Sci. Pt. A1* **1963**, 2155.

Sharples, A. Introduction to polymer crystallization. Edward Arnold: London, 1966; chap. 9.

Shuler, M. L.; Kargi, F., Bioprocess Engineering: Basic consepts. Prentice-Hall: New Jersey, **1992**; p. 80.

Smith, P.; Goulet, L., "Effect of the addition of amine diluents on the physical properties of poly(methyl methacrylate-co-methacrylic acid) copolymers obtained by partial hydrolysis of PMMA," *J. Polym. Sci. Pol. Phys.* **1993**, *31*, 327.

Sundararajan, P. R., Theta temperatures. In: Mark, J. E. editor. Physical properties of polymers handbook. AIP press: New York, 1996; p. 197-226.

Van Krevelen, D. W.; Hoftyzer, P. J. Properties of polymers, 2nd ed. Elsevier:Amsterdam, 1976; chap. 7.

Wang, Q.; Xu, X., "Structure and properties of p(MMA-MAA) PEO intermacromolecular complex formed through hydrogen-bonding," *Sci. China. Ser. B.* **1991**, *34*, 1409.

Wanka, G.; Hoffmann, H.; Ulbricht, W., "Phase diagrams and aggregation behavior of poly(oxyethylene)-poly(oxypropylene)-poly(oxyethylene) triblock copolymers in aqueous solutions," *Macromolecules* **1994**, *27*, 4145.

Winey, K. I.; Thomas, E. L.; Fetters, L. J., "The ordered bicontinuous double-diamond morphology in diblock copolymer/homopolymer blends," *Macromolecules* **1992**, *25*, 422.

Yoo, Y.; Kim, D.-C.; Kim, T.-Y., "Preparation and characterization of enalapril maleate-loaded nanoparticles using amphiphilic diblock copolymers," *J. Appl. Polym. Sci.* **1999**, *74*, 2856.

Yuan, Q. W. In *Polymer Data Handbook*, Mark, J. E., Ed.; Oxford University Press: New York, 1999, p. 548.

Yu, Z.; Liu, L., "Microwave-assisted synthesis of poly(ε-caprolactone)-poly(ethylene glycol)-poly(ε-caprolactone) tri-block co-polymers and use as matrices for sustained delivery of ibuprofen taken as model drug," *J. Biomater. Sci. Polym. Ed.* **2005**, *16*, 957.

Zalusky, A. S.; Olayo-Valles, R.; Wolf, J. H.; Hillmyer, M. A., "Ordered nanoporous polymers from polystyrene-polylactide block copolymers," *J. Am. Chem. Soc.* **2002**, *124*, 12761.

Zhao, Y.; Hu, T.; Lv, Z.; Wang, S.; Wu, C., "Laser light-scattering studies of poly(caprolactone-*b*-ethylene oxide-*b*-caprolactone) nanoparticles and their enzymatic biodegradation," *J. Polym. Sci. B.* **1999**, *37*, 3288.

Zhao, Y.; Liang, H.; Wang, S.; Wu, C., "Self-assembly of poly(caprolactone-*b*-ethylene oxide-*b*-caprolactone) via a microphase inversion in water," *J. Phys. Chem. B.* **2001**, *105*, 848.